is currently investigated for its potential as a therapeutic agent in bladder cancer. In RT112 cells that showed synergism of dicoumarol with cisplatin, cell viability decreased with the combination of dicoumarol with doxorubicin dose-dependently similarly to the case of cisplatin, but there was no effect in the case of paclitaxel (Fig. 1A). To confirm the effect of dicoumarol in enhancing doxorubicin-induced cytotoxicity, Trypan blue staining and Hoechst 33342 nuclear staining were used and showed that the combined treatment decreased cell viability by up to 45% of the control and increased apoptotic cells significantly compared with doxorubicin single treatment ($P < 0.01$). For doxorubicin and cisplatin, dicoumarol suppressed doxorubicin- or cisplatin-induced expression of p53/p21 and evoked PARP cleavage, whereas paclitaxel was unable to induce p53 accumulation and underwent its cytotoxicity through a p53-independent pathway (Fig. 1B). These results suggest that dicoumarol might enhance the cytotoxicity of genotoxic agents that activate the p53 pathway by modulating the interaction between NQO1 and p53.

FIG. 1. The synergistic effect of dicoumarol with chemotherapeutic agents against bladder cancer. ***A****, MTT assay showing the effects of dicoumarol on three kinds of chemotherapeutic agents, cisplatin (CDDP), doxorubicin (ADR) and paclitaxel, in RT112 cells. The results of MTT assays of RT112 treated by various agents at indicated concentrations only (green bar) or with dicoumarol at 100 μM (red bar) or 200 μM (orange bar) for 24 h are shown as the mean ± SD from three independent experiments. Cell viability is indicated by the ratio to cell viability when treated with only the drug vehicle.* ***B****, (i) Viable cell ratio examined by Trypan blue staining showing the combination effect of dicoumarol and ADR in RT112 cells. The results of Trypan blue staining with indicated treatments are shown as the mean ± SD. (ii) Apoptotic cell ratio examined by Hoechst 33342 staining showing the combined effect of dicoumarol and ADR in RT112 cells. The results of Hoechst 33342 staining with indicated treatments are shown as mean values ± SD, *P < 0.001 (two-sided t-tests).* ***C****, Western blot analysis showing the effects of dicoumarol on three kinds of chemotherapeutic agents (CDDP, ADR and paclitaxel) in RT112 cells. RT112 cells were treated with each chemotherapeutic agent for 12 h, with or without 1 h pretreatment with 100 μM dicoumarol, and then underwent Western blot analysis.*

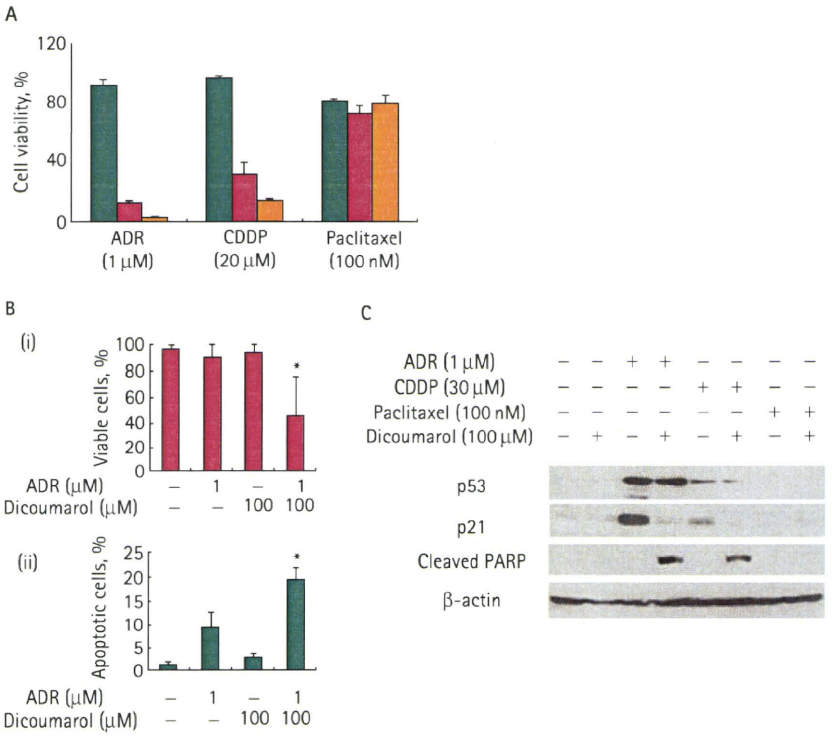

DICOUMAROL PROMOTES DOXORUBICIN-INDUCED APOPTOSIS IN BLADDER CANCER CELLS WITH FUNCTIONAL p53

To examine the importance of functional p53 for dicoumarol to enhance doxorubicin-induced cytotoxicity, the susceptibility of several other bladder cancer cell lines with different p53 statuses to doxorubicin and dicoumarol was monitored by MTT assay. Among the six bladder cancer cell lines, only RT112 cells have heterozygous polymorphism of NQO1, in which C changes to T at position 609 of the cDNA, leading to a change in the amino acid structure of the enzyme. Other cell lines have no polymorphism. All cell lines express NQO1 protein, although RT112 cells expressed relatively low levels of NQO1 protein compared with other cell lines (Fig. 2A). From the MTT assay dicoumarol enhanced doxorubicin-induced cytotoxicity in bladder cancer cell lines with wt-p53 such as RT112, 253J and KK47 (nine times, three times and 13 times against doxorubicin single treatment, respectively), but had no synergistic effect on doxorubicin in three cell lines with mt-p53 (TCCsup, EJ and J82) (Fig. 2A). We could not detect any correlation between NQO1 protein level and the effect of dicoumarol. To elucidate the necessity of functional p53 for synergism, two stable clones transfected with p53DN mutant (RT112 p53DN-2 and -11) were established. Although the antiproliferative effect of dicoumarol itself was not significantly changed by p53DN transfection, MTT assay showed that the effect of dicoumarol in enhancing the susceptibility to doxorubicin was weakened in both p53DN transfectants (Fig. 2A). Also, using Western blot analysis, the combination of doxorubicin and dicoumarol activated caspases in RT112 pCMVneo but not in RT112 p53DN-11 (Fig. 2B), and the inhibition of caspase activity by specific caspase inhibitors in RT112 pCMVneo suppressed the synergistic effect of dicoumarol (Fig. 2C). These results indicate that functional p53 is necessary for dicoumarol to enhance doxorubicin-induced apoptosis in urothelial cancer cells.

DICOUMAROL ENHANCED DOXORUBICIN-INDUCED CYTOTOXICITY VIA ACTIVATION OF THE p38 SIGNALLING PATHWAY IN BLADDER CANCER WITH wt-p53

The activation of mitogen-activated protein kinase (MAPK) cascades is considered to be one of the mechanisms by which chemotherapeutic agents induce apoptosis [7,8]. Whereas we have previously reported that dicoumarol activated the JNK pathway when used with cisplatin [5], the influence of dicoumarol on MAPK cascades when used with doxorubicin was investigated in the

*FIG. 2. The acceleration of doxorubicin (ADR)-induced apoptosis by dicoumarol in urothelial cancer cells with wt-p53 through a caspase-dependent pathway. **A**, The effects of dicoumarol on ADR-induced cytotoxicity assessed by the status of p53 and NQO1, using six urothelial cancer cell lines and two stable clones of RT112 transfected with p53 dominant-negative mutants (RT112 p53DN-2 and RT112 p53DN-11). The results of MTT assays with 1 μM ADR with or without 100 μM dicoumarol are shown as mean values ± SD from three independent experiments. **B**, Comparison of the response to ADR and dicoumarol between RT112 control transfectants (RT112 mock) and p53DN transfectant (RT112 p53DN-11), shown by Western blot analysis. Cells were treated with 1 μM ADR for 12 h, with or without 1 h pretreatment of 100 μM dicoumarol, and then lysed in RIPA buffer and subjected to Western blot analysis. **C**, The inhibiting effect of caspase inhibitors on dicoumarol-mediated enhancement of ADR-induced cytotoxicity in RT112 cells. Cells were pretreated with or without 100 μM dicoumarol for 1 h, followed by treatment with either ADR alone or ADR plus 80 μM Z-IETD-FMK (caspase-8 inhibitor), 100 μM Z-LEHD-FMK (caspase-9 inhibitor) or Z-VAD(OMe)-FMK (pan-caspase inhibitor), respectively, for an additional 24 h. Cell viability is indicated by the ratio to cell viability when treated with ADR alone. *P < 0.01 (two-sided t-test) vs ADR/dicoumarol combined therapy.*

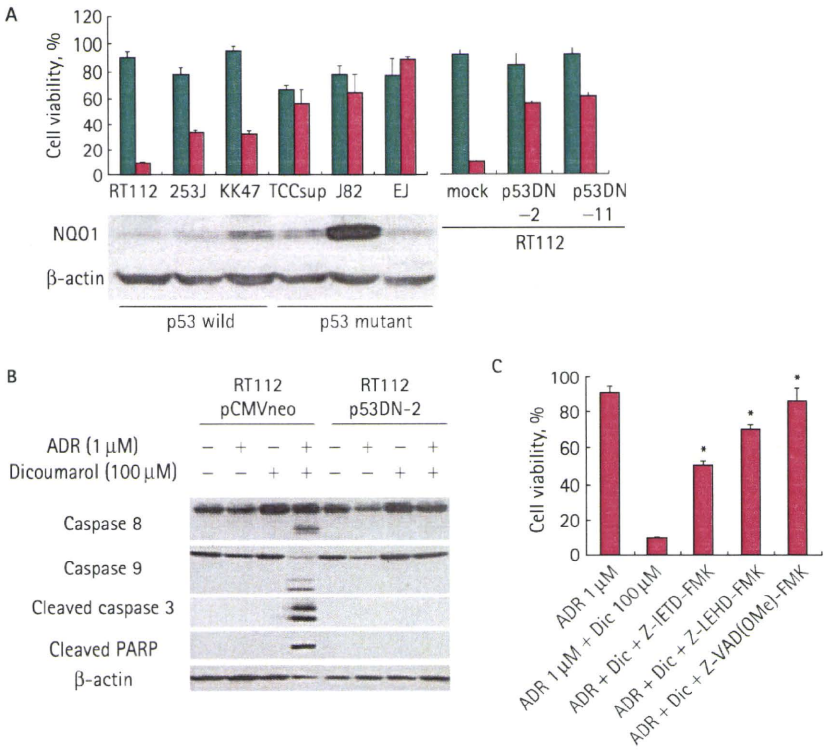

present study. The doxorubicin/dicoumarol combined treatment attenuated p53/p21 induction in the same manner as the cisplatin/dicoumarol combination. Among MAPK pathways, phosphorylation of p38 was more strongly induced 9 h after the treatment, although the expression levels of p38 were not changed (Fig. 3A).

To investigate the significance of p38 activation in the present experiments, RT112 cells were treated with SB202190, a specific inhibitor of p38. Although SB202190 (30 μM) alone slightly increased the cytotoxicity of doxorubicin, pretreatment with SB202190 apparently attenuated the effects of dicoumarol to enhance doxorubicin-induced cytotoxicity (Fig. 3B). On the other hand, SP600125, a specific JNK inhibitor, did not suppress apoptosis induced by doxorubicin/dicoumarol combined treatment (data not shown). The doxorubicin/dicoumarol combined treatment did not change the expression of Bax, Bcl-2 or Bcl-xL, but suppressed the expression of Mcl-1, which is one of the anti-apoptotic BH3 proteins. The inhibition of p38 activation by SB202190 restored Mcl-1 expression, and suppressed activation of caspase 3 (Fig. 3B). These findings suggest that dicoumarol enhanced the cytotoxicity of doxorubicin via activation of the p38 signalling pathway.

p21 ATTENUATION BY DICOUMAROL CONTRIBUTED TO PROMOTE p38 ACTIVATION IN UROTHELIAL CANCER CELLS WITH wt-p53

We examined the relationship between p53 status and the effect of dicoumarol to activate p38. The change of p38 status was examined in RT112 p53DN or other urothelial cancer cell lines after each drug exposure. The suppression of p53 function by p53DN attenuated p38 activation in RT112 cells (Fig. 4A). There were similar tendencies in 253J cells that retain wt-p53 and J82 cells harbouring mt-p53 (Fig. 4B). In 253J cells, dicoumarol/doxorubicin combined treatment attenuated p53/p21 expression and induced p38 phosphorylation followed by apoptotic change. In contrast, in J82 cells, the normal function of the p53 gene was lost. There was no p21 induction after doxorubicin exposure, and dicoumarol/doxorubicin combined treatment did not induce the phosphorylation of p38. These results indicate that dicoumarol could evoke p38 activation only in cancer cells with wt-p53.

To confirm whether the suppression of p21 expression by dicoumarol contributed to enhance doxorubicin-induced cytotoxicity via p38 activation, we established a stable clone of RT112 transfected with a p21siRNA vector (RT112 p21siRNA-8) and investigated the p38 status and susceptibility to doxorubicin. The suppression of p21 expression made RT112 cells about six times more susceptible to doxorubicin in MTT assay and, at that time, the p38 signalling pathway was activated and Mcl-1 expression was suppressed (Fig. 4C). All together, these results indicate that p21 attenuation by dicoumarol contributed to p38 activation and enhancement of doxorubicin-induced cytotoxicity in urothelial cancer cells with wt-p53.

DISCUSSION

Due to its up-regulation in tumour lesions, NQO1 has been considered a good molecular target in bladder cancer. Mitomycin C and its structurally related compound EO9, which are activated by NQO1, have shown their effectiveness as intravesically instilled agents, although the relationship between the response and NQO1 is still controversial [9,10]. In the present study, we used dicoumarol, an inhibitor of the enzymatic activity of NQO1,

and showed that it contributed to enhance doxorubicin-induced cytotoxicity through p38 activation in urothelial cancer cells with wt-p53.

NQO1 has a function to stabilize p53 protein. NQO1 inhibition by dicoumarol therefore induced p53 degradation and was reported to block wt-p53-mediated apoptosis induced by γ-irradiation [11]. However, p53-dependent p21 induction has recently been considered to inhibit the apoptotic response, and p21 attenuation has the potential to make genotoxic chemotherapeutic agents more effective [12,13]. Although p53 mutation has an important role in bladder cancer invasion and progression, most low to intermediate risk superficial bladder cancers retain wt-p53 and intravesical treatment with genotoxic agents such as doxorubicin could not show sufficient effectiveness. If this resistance against doxorubicin may even partially come from chemoresistant mechanism of p53-p21 pathway, we think that the combination of dicoumarol can be useful to enhance its effect in bladder cancer.

The present results showed that the combination of dicoumarol with genotoxic agents suppresses p21 induction by functional p53 and simultaneously evokes the stress-activated protein kinase (SAPK) family such as JNK and p38 signalling pathways, resulting in the induction of apoptosis. We think that mechanisms between p21 suppression and the activation of SAPK family should be further elucidated in various cell lines, because p53 mutant cell lines such as RT112 p53DN and J82 did not show p38 activation after doxorubicin or doxorubicin/dicoumarol treatment although they had already lost p21 inducibility. Concerning the anticancer effect of dicoumarol, several reports have referred to its effect to induce oxidative stress [14,15], and intracellular reactive oxygen species status is also important to activate SAPK family [16]. We now speculate that p21 attenuation is one of the mechanisms of dicoumarol to activate SAPK family but other additional effects of dicoumarol are also necessary to activate SAPK family.

The present results showed the possibility that the Mcl-1 protein may be a downstream molecule regulated by the p38 signalling pathway. Mcl-1 decreased when apoptosis was induced with p38 activation, and inhibition of p38 activation by SB202190 restored the Mcl-1 protein level. Mcl-1 is an anti-apoptotic Bcl-2 family member. Several studies have shown that Mcl-1 plays a particularly important functional role in promoting survival in malignant haematopoietic cells, including leukaemia and myeloma cells, although there has been no report on its role in urothelial cancer [17,18]. Recently, the possibility was suggested that p38 MAPK may positively or negatively regulate Mcl-1 stability and turnover [19], and therefore, we propose that the suppression of Mcl-1 protein by p38 activation may have a crucial role in the doxorubicin/dicoumarol combined treatment. We would like to further elucidate the importance of this pathway in the apoptotic process of urothelial cancer in the future.

In conclusion, in the present study dicoumarol sensitized urothelial cancer cells with wt-p53 to doxorubicin through p38 activation induced by the suppression of the p53/p21 pathway. Most low to intermediate risk superficial bladder cancers retain wt-p53, and we think that the present results will provide a new strategy to overcome rapid or frequent recurrence of such superficial bladder cancers after conventional intravesical instillation therapy. In those cancers with wt-p53, we think that the risk of transient combined therapy leading to selective progression of p53-mutant cancer cells may be low, although we have to pay attention to this possibility in clinical setting. Furthermore, because dicoumarol enhanced cisplatin- and doxorubicin-induced cytotoxicity through different MAPK cascades, a concomitant use of dicoumarol may effectively enhance the cytotoxicity of conventional multi-drug combined chemotherapy such as methotrexate, vinblastine, doxorubicin and cisplatin (MVAC), and cisplatin, methotrexate and vinblastine (CMV) for invasive TCC. We are planning to start the evaluation of its efficacy and safety in an *in vivo* orthotopic or metastatic mouse model.

FIG. 3. Dicoumarol promotes doxorubicin (ADR)-induced apoptosis via activation of the p38 signalling pathway. ***A****, Western blot analysis showing changes of the p53-p21 pathway and the MAPK cascade in RT112 treated with ADR with or without dicoumarol. Cells were treated with 1 μM ADR for 12 h, with or without 1 h pretreatment of 100 μM dicoumarol. '0 h' refers to the time of ADR addition.* ***B****, MTT assay (upper panel) and Western blot analysis (lower panel) showing the effect of inhibition of the p38 signalling pathway on dicoumarol-mediated enhancement of ADR-induced apoptosis in RT112. MTT assays with 1 μM ADR with or without 100 μM dicoumarol and/or 30 μM SB202190 are shown as mean values ± SD from three independent experiments. *P < 0.01 (two-sided t-test) vs ADR/dicoumarol and ADR/dicoumarol/SB202190. The status of molecules associated with apoptosis in RT112 treated with ADR, dicoumarol and SP202190, a p38 specific inhibitor, are shown in Western blot analysis after cells were treated with the indicated drugs for 12 h.*

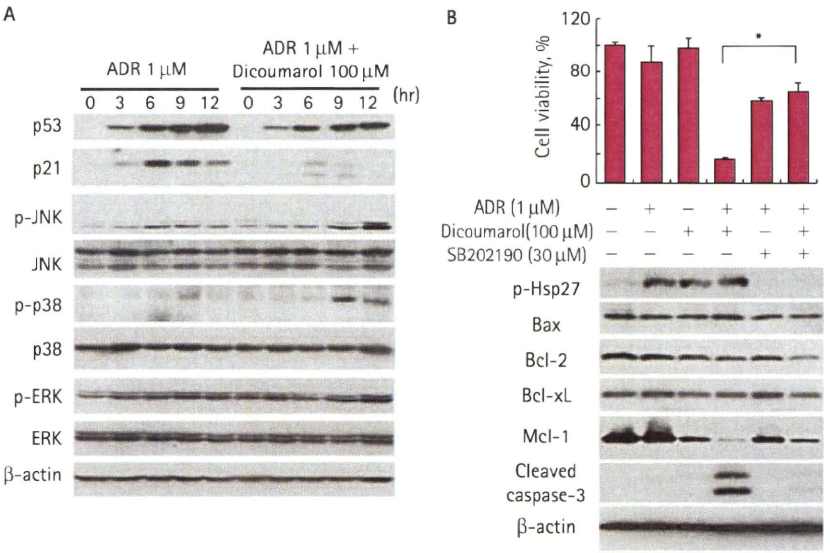

CONFLICT OF INTEREST

None declared.

*FIG. 4. Dicoumarol activates the p38 signalling pathway in p53 wt-cells via p21 attenuation. **A**, Comparison of p38 status between RT112 control transfectants (RT112 mock) and p53DN transfectant (RT112 p53DN-11) treated with doxorubicin (ADR) and dicoumarol, shown by Western blot analysis. Cells were treated with 1 μM ADR for 12 h, with or without 1 h pretreatment of 100 μM dicoumarol, and then lysed in RIPA buffer and subjected to Western blot analysis. **B**, Western blot analysis showing changes in the p53-p21 pathway and p38 phosphorylation in 253J cells (wt-p53) and J82 cells (mt-p53) treated with ADR with or without dicoumarol. Cells were treated with the indicated drugs for 12 h, and then lysed in RIPA buffer and subjected to Western blot analysis. **C**, MTT assay (upper panel) and Western blot analysis (lower panel) showing the induction of p38 activation and apoptosis by the attenuation of p21 expression. RT112 cells stably transfected with control vector (RT112 mock) or p21siRNA vector (RT112 p21siRNA-8) were treated with 1 μM ADR for 12 h, and then p53 and p21 expression, p38 phosphorylation, Mcl-1 and cleaved caspase 3 were examined in Western blot analysis. Cell viability was examined by MTT assay 24 h after the treatment.*

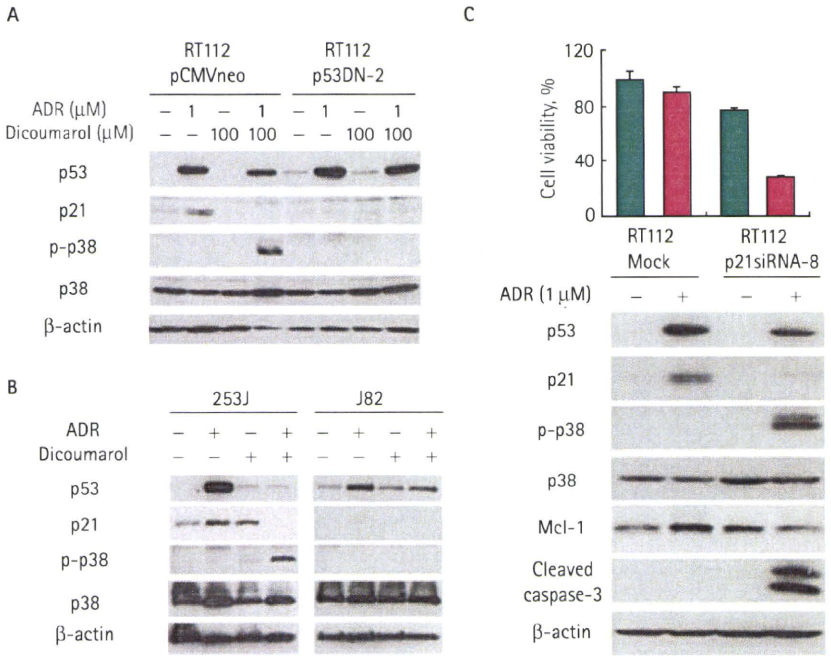

REFERENCES

1 **Yoshimura K, Utsunomiya N, Ichioka K, Matsui Y, Terai A, Arai Y.** Impact of superficial bladder cancer and transurethral resection on general health-related quality of life: an SF-36 survey. *Urology* 2005; **65**: 290–4

2 **Witjes JA, Hendricksen K.** Intravesical pharmacotherapy for non-muscle-invasive bladder cancer: a critical analysis of currently available drugs, treatment schedules, and long-term results. *Eur Urol* 2008; **53**: 45–52

3 **Siegel D, Gustafson DL, Dehn DL *et al.*** NAD(P)H: quinone oxidoreductase 1: role as a superoxide scavenger. *Mol Pharmacol* 2004; **65**: 1238–47

4 **Danson S, Ward TH, Butler J, Ranson M.** DT-diaphorase: a target for new anticancer drugs. *Cancer Treat Rev* 2004; **30**: 437–49

5 **Watanabe J, Nishiyama H, Matsui Y *et al.*** Dicoumarol potentiates cisplatin-induced apoptosis mediated by c-Jun N-terminal kinase in p53 wild-type urogenital cancer cell lines. *Oncogene* 2006; **25**: 2500–8

6 **Watanabe J, Nishiyama H, Okubo K *et al.*** Clinical evaluation of p53 mutations in urothelial carcinoma by IHC and FASAY. *Urology* 2004; **63**: 989–93

7 **Eom YW, Kim MA, Park SS *et al.*** Two distinct modes of cell death induced by doxorubicin: apoptosis and cell death through mitotic catastrophe accompanied by senescence-like phenotype. *Oncogene* 2005; **24**: 4765–77

8 **Mansouri A, Ridgway LD, Korapati AL *et al.*** Sustained activation of JNK/p38 MAPK pathways in response to cisplatin leads to Fas ligand induction and cell death in ovarian carcinoma cells. *J Biol Chem* 2003; **278**: 19245–56

9 **Choudry GA, Stewart PA, Double JA *et al.*** A novel strategy for NQO1 (NAD(P)H: quinone oxidoreductase, EC 1.6.99.2) mediated therapy of bladder cancer based on the pharmacological properties of EO9. *Br J Cancer* 2001; **85**: 1137–46

10 **Puri R, Palit V, Loadman PM *et al.*** Phase I/II pilot study of intravesical apaziquone (EO9) for superficial bladder cancer. *J Urol* 2006; **176**: 1344–8

11 **Asher G, Lotem J, Cohen B, Sachs L, Shaul Y.** Regulation of p53 stability and p53-dependent apoptosis by NADH quinone oxidoreductase 1. *Proc Natl Acad Sci USA* 2001; **98**: 1188–93

12 **Gartel AL, Tyner AL.** The role of the cyclin-dependent kinase inhibitor p21 in apoptosis. *Mol Cancer Ther* 2002; **1**: 639–49

13 **Weiss RH.** p21Waf1/Cip1 as a therapeutic target in breast and other cancers. *Cancer Cell* 2003; **4**: 425–9

14 **Bello RI, Gomez-Diaz C, Lopez-Lluch G *et al.*** Dicoumarol relieves serum withdrawal-induced G0/1 blockade in HL-60 cells through a superoxide-dependent mechanism. *Biochem Pharmacol* 2005; **69**: 1613–25

15 **Du J, Daniels DH, Asbury C *et al.*** Mitochondrial production of reactive oxygen species mediate dicumarol-induced cytotoxicity in cancer cells. *J Biol Chem* 2006; **281**: 37416–26

16 **Matsuzawa A, Ichijo H.** Redox control of cell fate by MAP kinase: physiological roles of ASK1-MAP kinase pathway in stress signaling. *Biochim Biophys Acta* 2008; **1780**: 1325–36

17 **Le Gouill S, Podar K, Harousseau JL, Anderson KC.** Mcl-1 regulation and its role in multiple myeloma. *Cell Cycle* 2004; **3**: 1259–62

18 **Zhou P, Qian L, Kozopas KM, Craig RW.** Mcl-1, a Bcl-2 family member, delays the death of hematopoietic cells under a variety of apoptosis-inducing conditions. *Blood* 1997; **89**: 630–43

19 **Derouet M, Thomas L, Moulding DA *et al.*** Sodium salicylate promotes neutrophil apoptosis by stimulating caspase-dependent turnover of Mcl-1. *J Immunol* 2006; **176**: 957–65

Correspondence: Hiroyuki Nishiyama, Department of Urology, Graduate School of Medicine, Kyoto University, Kyoto 606-8507, Japan.
e-mail: nishiuro@kuhp.kyoto-u.ac.jp

Abbreviations: **(MA)(SA)PK**, (mitogen-activated) (stress-activated) protein kinase; **p53DN**, dominant-negative mutant of p53; **shRNA**, short hairpin RNA; **Mcl-1**, myeloid cell leukaemia 1; **NQO1**, NADPH: quinone oxidoreductase 1; **(wt)(mt)-p53**, (wild-type) (mutant) p53; **MTT**, 3-(4, 5-dimethylthiazol-2-yl)-2, 5-diphenyltetrazolium bromide assay; **PARP**, poly(ADP-ribose) polymerase; **JNK**, c-Jun amino-terminal kinase.

British Journal of Cancer (2010) 102, 883–891

www.bjcancer.com

miR-145 and *miR-133a* function as tumour suppressors and directly regulate FSCN1 expression in bladder cancer

T Chiyomaru[1], H Enokida[*,1], S Tatarano[1], K Kawahara[2], Y Uchida[1], K Nishiyama[1], L Fujimura[3], N Kikkawa[4], N Seki[4] and M Nakagawa[1]

[1]Department of Urology, Graduate School of Medical and Dental Sciences, Kagoshima University, Kagoshima, Japan; [2]Kawahara Nephro-urology Clinic, Kagoshima, Japan; [3]Biomedical Research Center, Chiba University, Chiba, Japan; [4]Department of Functional Genomics, Graduate School of Medicine, Chiba University, Chiba, Japan

BACKGROUND: We have recently identified down-regulated microRNAs including *miR-145* and *miR-133a* in bladder cancer (BC). The aim of this study is to determine the genes targeted by *miR-145*, which is the most down-regulated microRNA in BC.
METHODS: We focused on *fascin homologue 1* (*FSCN1*) from the gene expression profile in *miR-145* transfectant. The luciferase assay was used to confirm the actual binding sites of *FSCN1* mRNA. Cell viability was evaluated by cell growth, wound-healing, and matrigel invasion assays. BC specimens were subjected to immunohistochemistry of FSCN1 and *in situ* hybridisation of *miR-145*.
RESULTS: The *miR-133a* as well as *miR-145* had the target sequence of *FSCN1* mRNA by the database search, and both microRNAs repressed the mRNA and protein expression of FSCN1. The luciferase assay revealed that *miR-145* and *miR-133a* were directly bound to *FSCN1* mRNA. Cell viability was significantly inhibited in *miR-145*, *miR-133a*, and si-FSCN1 transfectants. *In situ* hybridisation revealed that *miR-145* expression was markedly repressed in the tumour lesion in which FSCN1 was strongly stained. The immunohistochemical score of FSCN1 in invasive BC ($n=46$) was significantly higher than in non-invasive BC ($n=20$) ($P=0.0055$).
CONCLUSION: Tumour suppressive *miR-145* and *miR-133a* directly control oncogenic FSCN1 in BC.
British Journal of Cancer (2010) **102,** 883–891. doi:10.1038/sj.bjc.6605570 www.bjcancer.com
Published online 16 February 2010

Keywords: FSCN1; microRNA; *miR-145*; *miR-133a*; bladder cancer

Bladder cancer (BC) is the fifth most common cancer in the United States and the second most common cancer of the genitourinary tract (Parkin *et al*, 2005; Jemal *et al*, 2008). In Japan, the age-standardised mortality rate of BC has increased slightly since 1993 (Qiu *et al*, 2009). Currently, the standard diagnostic method depends on the use of invasive urethro-cystoscopy. Bladder tumour antigen and nuclear matrix protein-22 are available as urine markers for BC diagnostic tools. However, they are not widely used because of their low sensitivity and specificity for distinguishing BC from non-malignant diseases (van Rhijn *et al*, 2005). In the treatment of BC, morphologically similar tumours can behave differently, and it is currently not possible to identify patients who will experience tumour recurrence or disease progression (Kwak *et al*, 2004). Therefore, a new diagnostic method and treatment based on BC biology are desired.

MicroRNAs are an abundant class of small non-coding RNAs of about 22 nucleotides in length that function as negative regulators of gene expression through antisense complimentarily to specific messenger RNAs (Lagos-Quintana *et al*, 2001). Although their biological functions remain largely unknown, recent studies suggest that microRNAs contribute to the development of various cancers (Schickel *et al*, 2008). The *miR-145* and *miR-133a/b* have been commonly identified as down-regulated in the microRNA expression signatures of various human malignancies: head and neck carcinoma (Wang *et al*, 2008; Wong *et al*, 2008a; Childs *et al*, 2009), pancreatic ductal adenocarcinoma (Szafranska *et al*, 2007), lung cancer (Liu *et al*, 2009), breast cancer (Sempere *et al*, 2007; Wang *et al*, 2009a), gastric cancer (Takagi *et al*, 2009), colorectal cancer (Bandrés *et al*, 2006; Slaby *et al*, 2007; Schepeler *et al*, 2008; Wang *et al*, 2009b), prostate cancer (Ozen *et al*, 2008; Tong *et al*, 2009), and BC (Friedman *et al*, 2009; Lin *et al*, 2009a). In our microRNA screening test of BC, we identified a subset of seven differentially down-regulated microRNAs (*miR-145*, *miR-133a*, *miR-133b*, *miR-30a-3p*, *miR-195*, *miR-125b*, and *miR-199a**) among the 156 microRNAs examined, and *miR-145* was the most down-regulated one of all (Ichimi *et al*, 2009). These studies strongly suggest that low expression levels of *miR-145* and *miR-133a/b* may contribute to pathogenesis and progression of human malignancies. Moreover, functional analyses of target genes, which are repressed by these microRNAs, are crucial to elucidate the mechanisms of cancer development. In this study, we performed an oligo-microarray analysis of *miR-145*-transfected BC cell lines in comparison with their parental cell lines for genome-wide screening of target genes silenced by *miR-145* in BC, and we found that *fascin homologue 1* (*FSCN1*) was the most down-regulated one among the genes.

FSCN1 is an actin-binding protein required for the formation of actin-based cell-surface protrusions and cytoplasmic bundles of

*Correspondence: Dr H Enokida, Department of Urology, Graduate School of Medical and Dental Sciences, Kagoshima University, 8-35-1 Sakuragaoka, Kagoshima 890-8520, Japan;
E-mail: enokida@m.kufm.kagoshima-u.ac.jp
Received 18 November 2009; revised 12 January 2010; accepted 18 January 2010; published online 16 February 2010

microfilaments (Hashimoto *et al*, 2005). FSCN1 activity is essential to filopodial dynamics, and it has been proposed that fascin imparts rigidity to the forming filopodia to efficiently push the membrane forwards (Vignjevic *et al*, 2006). Cells with prominent cytoplasmic protrusions and actively migrating cells express high levels of FSCN1, whereas this protein is undetectable in most normal epithelial cells (Pelosi *et al*, 2003). Over-expression of FSCN1 in a variety of tumours such as lung (Pelosi *et al*, 2003), prostate (Darnel *et al*, 2009), oesophageal (Zhang *et al*, 2006), breast (Grothey *et al*, 2000), colon (Jawhari *et al*, 2003), pancreas (Maitra *et al*, 2003), ovary (Lin *et al*, 2009b), and skin cancers (Goncharuk *et al*, 2002) usually correlates with high-grade, extensive invasion, distant metastasis, and poor prognosis. However, little is known about the function of FSCN1 in BC, and it is not known whether FCSN1 expression is regulated by specific microRNAs.

We hypothesised that *miR-145* and *miR-133a/b* directly regulate FSCN1 and that FSCN1 has oncogenic activity in BC. We used a luciferase reporter assay to determine whether FSCN1 actually has sites targeted by *miR-145* and *miR-133a*. To investigate the functional roles of FSCN1 in BC, we performed a loss-of-function study using BC cell lines. Furthermore, we evaluated FSCN1 protein expression in clinical BC specimens by immunohistochemistry.

MATERIALS AND METHODS

Clinical samples and cell culture

The tissue specimens were from 66 BC patients who had undergone cystectomy or transurethral resection of bladder tumours at Kagoshima University Hospital between 2001 and 2005. The patient's background and clinico-pathological characteristics are summarised in Table 1. These samples were staged according to the American Joint Committee on Cancer-Union Internationale Contre le Cancer tumour-node-metastasis classification and histologically graded (Sobin and Wittekind, 2002). Normal bladder epithelia (N1 and N2) were derived from patients with non-cancerous disease and were used as the controls. Our study was approved by the Bioethics Committee of Kagoshima University; written prior informed consent and approval were given by the patients. We used three human BC cell lines; BOY was established in our laboratory from an Asian male patient aged 66 years, who had a diagnosis of stage III BC with lung metastasis (Ichimi *et al*, 2009); T24 was obtained from American Type Culture Collection; and KK47 was established in Kanazawa University and kindly provided. These cell lines were maintained in a minimum essential medium (MEM) supplemented with 10% foetal bovine serum in a humidified atmosphere of 5% CO_2 and 95% air at 37°C.

Table 1 Patient characteristics

Total number	**66**
Gender	
Male	51
Female	15
Age	
Median age (range)	72 (47–92) years
Stage	
Superficial (pTa)	20
Invasive (⩾pT1)	46
Grade	
G1	7
G2	41
G3	18
Operation	
Cystectomy	17
TUR-BT	49
Recurrence	
Yes	38
No	28

Abbreviation: TUR-BT = transurethral resection of bladder tumour.

Mature microRNA and siRNA transfection

As earlier described (Ichimi *et al*, 2009), the transfection of BC cell lines was accomplished with RNAiMAX transfection reagent (Invitrogen, Carlisbad, CA, USA), Opti-MEM (Invitrogen) with 10 nM of mature microRNA molecules. For gain-of-function experiments, we used Pre-miR and negative-control microRNA (Applied Biosystems, Foster City, CA, USA), whereas *FSCN1* siRNA (LU-019576-00, J-019576-07, J-019576-08; Thermo Fisher Scientific, Waltham, MA, USA) and negative-control siRNA (D-001810-10; Thermo Fisher Scientific) were used for loss-of-function experiments. Cells were seeded under the following conditions: 800 000 in a 10 cm dish for protein extraction, 3000 per well in a 96-well plate for XTT assay, 200 000 per well in a 6-well plate for the wound-healing assay, and 50 000 per well in a 24-well plate for the mRNA extraction, matrigel invasion assay, and luciferase assay.

Quantitative real-time RT-PCR

TaqMan probes and primers for FSCN1 (P/N: Hs00979631_g1; Applied Biosystems) were assay-on-demand gene expression products. All reactions were performed in duplicate and a negative-control lacking cDNA was included. Regarding the PCR conditions, we followed the manufacturer's protocol. Stem-loop RT-PCR (TaqMan MicroRNA Assays; Applied Biosystems) was used to quantitate microRNAs according to the earlier published conditions (Ichimi *et al*, 2009). For quantitative analysis of *FSCN1* mRNA and the microRNAs, *human 18s rRNA* (P/N: Hs99999901_s1; Applied Biosystems) and *RNU48* (P/N: 001006; Applied Biosystems), respectively, served as internal controls, and the delta-delta Ct methods to calculate the fold change. We used premium total RNA from normal human bladder (Clontech, Mountain View, CA, USA) as a reference.

Gene expression analysis of BC cell lines

Total RNA was extracted by using TRIzol (Invitrogen) according to the manufacturer's protocol. The integrity of the RNA was checked with an RNA 6000 Nano Assay kit and 2100 Bioanalyzer (Agilent Technologies, Santa Clara, CA, USA). Oligo-microarray Human 44K (Agilent Technologies) was used for expression profiling in *miR-145*-transfected BC cell lines (T24 and KK47) in comparison with miR-negative-control transfectant, as described earlier (Sugimoto *et al*, 2009). Briefly, hybridisation and washing steps were performed in accordance with the manufacturer's instructions. The arrays were scanned using a Packard GSI Lumonics ScanArray 4000 (Perkin Elmer, Boston, MA, USA). The data obtained were analysed by means of DNASIS array software (Hitachi Software Engineering), which converted the signal intensity for each spot into text format. The Log2 ratios of the median subtracted background intensity were analysed. Data from each microarray study were normalised by the global normalisation method.

Western blots

After 3 days of transfection, protein lysate (50 μg) was separated by NuPAGE on 4–12% bis-tris gel (Invitrogen) and transferred into a polyvinylidene fluoride membrane. Immunoblotting was carried

out with diluted (1:100) monoclonal FSCN1 antibody (ab49815, Abcam, Cambridge, UK) and GAPDH antibody (MAB374; Chemicon, Temecula, CA, USA). The membrane was washed and then incubated with goat anti-mouse IgG (H + L)-HRP conjugate (Bio-Rad, Hercules, CA, USA). Specific complexes were visualised with an echochemiluminescence detection system (GE Healthcare, Little Chalfont, UK).

Cell growth, wound-healing, and matrigel invasion assays

Cell growth was determined by using an XTT assay (Roche Applied Sciences, Tokyo, Japan) that was performed according to the manufacturer's instructions. Cell migration activity was evaluated by wound-healing assay. Cells were plated in six-well dishes, and the cell monolayer was scraped using a micropipette tip. The initial gap length (0 h) and the residual gap length 24 h after wounding were calculated from Photomicrographs. A cell invasion assay was carried out using modified Boyden Chambers consisting of transwell-precoated matrigel membrane filter inserts with 8 μm pores in 24-well tissue culture plates (BD Biosciences, Bedfold, MA, USA). MEM containing 10% foetal bovine serum in the lower chamber served as the chemoattractant. All experiments were performed in triplicate.

Prediction of microRNA targets

To investigate the predicted target genes and their conserved sites in which the seed region of each microRNA binds, we used the TargetScan program (release 5.0, http://www.targetscan.org/). The sequences of the predicted mature microRNAs were confirmed by referring miRBase (release 13.0, http://microrna.sanger.ac.uk/).

Plasmid construction and dual-luciferase assay

MicroRNA target sequences were inserted between the XhoI–PmeI restriction sites in the 3′-UTR of the hRluc gene in psiCHECK-2 vector (C8021, Promega, Madison, WI, USA). BOY cells were transfected with 5 ng of vector, 10 nM of microRNAs, and 1 μl of Lipofectamine 2000 (Invitrogen) in a 100 μl Opti-MEM. The activities of firefly and *Renilla* luciferases in cell lysates were determined with a dual-luciferase assay system (Promega). Normalised data were calculated as the quotient of *Renilla*/firefly-luciferase activities.

Immunohistochemistry

The primary mouse monoclonal antibodies against FSCN1 (Abcam) were diluted by 1:200. The slides were treated with Biotinylated Anti-Mouse IgG (H + L) made in horse (Vector laboratories, Burlingame, CA, USA). Diaminobenzidine-hydrogen peroxide (Sigma-Aldrich, St Louis, MO, USA) was the chromogen, and the counterstaining was carried out with 0.5% haematoxylin. The positivity of endothelia and myofiblasts served as an inner positive control. The intensity of the staining was scored as negative (0), weak (1), moderate (2), or strong (3) (Ropponen *et al*, 1999). All staining scores are averages of duplicate experiments, and all samples were independently scored by two of us (TC and HE) who were blinded to the patient status.

In situ hybridisation of microRNA

In situ hybridisation was carried out according to the manufacturer's protocol for formalin-fixed, paraffin-embedded (FFPE) tissue (Kloosterman *et al*, 2006) on human BC specimens. DIG-labelled LNA oligo-nucleotides were purchased from EXIQON (Woburm, MA, USA) and used for overnight hybridisation at 52°C. The staining was carried out as described earlier. After deparaffinisation, the specimens were subjected to proteinase K (20 Ag per ml) digestion for 20 min. The post-fixed tissues were subsequently incubated overnight with the locked nucleic acid-modified probes. For the immunodetection, tissues were incubated overnight at 4°C in anti-DIG-AP FAB fragment (Roche Applied Sciences; 1/2000). The final visualisation was carried out with NBT/BCIP (Pierce, Rockford, IL, USA).

Statistical analysis

The relationship between two variables and the numerical values obtained by real-time RT–PCR was analysed using the Mann–Whitney *U*-test. The relationship between three variables and the numerical values was analysed using the Bonferroni-adjusted Mann–Whitney *U*-test. The analysis software was Expert StatView (version 4, SAS Institute Inc., Cary, NC, USA); for the comparison test among the three variables, a non-adjusted statistical level of significance of $P<0.05$ corresponds to a Bonferroni-adjusted level of $P<0.0167$.

RESULTS

Gene expression profile identifying down-regulated genes in *miR-145* transfectant

For genome-wide screening of target genes silenced by *miR-145* in BC, we performed an oligo-microarray analysis of *miR-145*-transfected BC cell lines (T24 and KK47) in comparison with miR-negative-control transfectant. A total of 200 genes were generally down-regulated by >0.5-fold in *miR-145* transfectants compared with the control. We focused on *FSCN1* because it was listed as the top candidate in the expression profile (Table 2).

FSCN1 as a target of post-transcriptional repression by *miR-145* and *miR-133a*

Among the T24 cell lines transfected with the six down-regulated microRNAs in our earlier study (Ichimi *et al*, 2009), the expression levels of *FSCN1* mRNA and its protein were markedly decreased not only in *miR-145*, but also in *miR-133a* transfectants (Figure 1A and B). We performed a luciferase assay to determine whether *FSCN1* mRNA actually has the target sites of these two microRNAs, as indicated by the TargetScan algorithm. We initially used the vector encoding full-length 3′-UTR of *FSCN1* mRNA (position 51–1180), and the luminescence intensity was significantly decreased in *miR-145* and *miR-133a* transfectants (Figure 2A). Furthermore, to determine the specific sites targeted by the two microRNAs, we constructed vectors covering four conserved sites for *miR-145* and one site for *miR-133a* (Figure 2B). The luminescence intensity was significantly decreased at the two sites targeted by *miR-145* (positions 377–383 and 1140–1146) and one site targeted by *miR-133a* (position 745–751) (Figure 2B). In addition, we constructed three mutated vectors in which the specific sites targeted by the microRNAs were deleted, and the luminescence intensity was not decreased at all by *miR-145* and *miR-133a* (Figure 2C). We did not examine *miR-133b* because it was considered to function similarly to *miR-133a*; these microRNAs have very similar sequences (*miR-133a*: UUGGUCCCCUUCAACCAGCUGU, *miR-133b*: UUGGUCCCCUUCAACCAGCUA) and have a common sequence for binding to *FSCN1* mRNA (UUGGUC) (Figure 2B).

Effect of *miR-145* and *miR-133a* transfection on cell growth, invasion, and migration activity in BC cell lines

The expression levels of *miR-145* and *miR-133a* were extremely low in the BC cell lines compared with normal bladder epithelia (N1 and N2) (Figure 3A), suggesting that endogenous *miR-145* or *miR-133a* in these cell lines does not affect cell viabilities. Therefore, we performed gain-of-function studies using the microRNA transfectants to investigate the functional role of *miR-145* and *miR-133a*. The XTT cell-growth assay showed significant cell-

Table 2 Top 20 genes that were down-regulated by >0.5-fold in *miR-145* transfectants in comparison with the control

Entrez gene ID	Gene symbol	Gene name	Log2 ratio
6624	FSCN1	Fascin homologue 1, actin-bundling protein (*Strongylocentrotus purpuratus*)	−3.95
10447	FAM3C	Family with sequence similarity 3, member C	−3.26
203547	LOC203547	Hypothetical protein LOC203547	−3.17
2519	FUCA2	Fucosidase, α-L-2, plasma	−2.88
51280	GOLM1	Golgi membrane protein 1	−2.85
56674	TMEM9B	TMEM9 domain family, member B	−2.85
5094	PCBP2	Poly(rC)-binding protein 2	−2.81
84841	MGC15634	Hypothetical protein MGC15634	−2.80
2764	GMFB	Glia maturation factor, β	−2.63
91452	ACBD5	Acyl-coenzyme A-binding domain containing 5	−2.61
7048	TGFBR2	Transforming growth factor, β receptor II (70/80 kDa)	−2.57
8508	NIPSNAP1	Nipsnap homologue 1 (*Caenorhabditis elegans*)	−2.55
23075	SWAP70	SWAP-70 protein	−2.54
92675	DTD1	D-tyrosyl-tRNA deacylase 1 homologue (*Saccharomyces cerevisiae*)	−2.53
27250	PDCD4	Programmed cell death 4 (neoplastic transformation inhibitor)	−2.52
57552	AADACL1	Arylacetamide deacetylase-like 1	−2.49
4697	NDUFA4	NADH dehydrogenase (ubiquinone) 1 α subcomplex, 4, 9 kDa	−2.46
5530	PPP3CA	Protein phosphatase 3 (formerly 2B), catalytic subunit, α isoform	−2.39
51199	NIN	Ninein (GSK3B-interacting protein)	−2.26
89894	TMEM116	transmembrane protein 116	−2.03

Abbreviation: NADH = nicotinamide adenine dinucleotide.

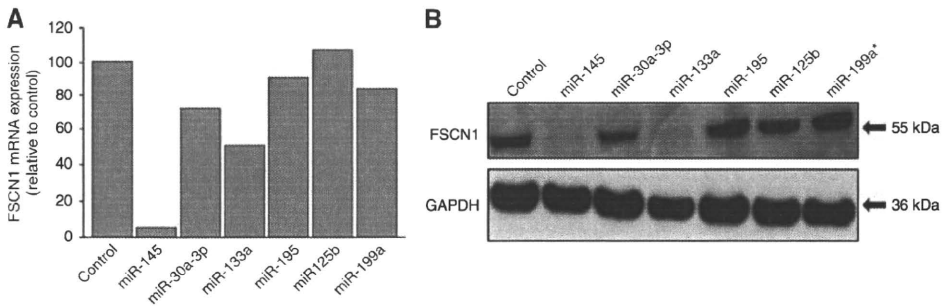

Figure 1 Regulation of FSCN1 expression in the down-regulated microRNA transfectants (T24). (**A**) *FSCN1* mRNA expression after 24 h transfection with 10 nM of microRNAs (*miR-145*, *miR-30a-3p*, *miR-133a*, *miR-195*, *miR-125b*, and *miR-199a**). *FSCN1* mRNA expression was repressed in *miR-145* and *miR-133a* transfectants. (**B**) FSCN1 protein expression after 72 h transfection of microRNAs. Glyceraldehyde-3-phosphate dehydrogenase (GAPDH) was used as a loading control. The protein expression level of FSCN1 was also repressed in the transfectants.

growth inhibitions in *miR-145* and *miR133a* transfectant compared with the controls from BOY and T24 cell lines (BOY, 86.6 ± 1.6, 65.7 ± 0.3, 100 ± 0.6, respectively, $P<0.0001$; and T24, 87.4 ± 0.6, 69.5 ± 1.5, 100 ± 0.9, respectively, $P<0.0005$; Figure 3B). The wound-healing assay showed significant cell migration inhibitions in *miR-145* and *miR133a* transfectant (BOY, 59.0 ± 3.5, 58.1 ± 3.4, 100.0 ± 2.4, respectively, $P<0.0001$; and T24, 74.5 ± 2.5, 72.3 ± 4.0, 100.0 ± 2.7, respectively, $P<0.0001$; Figure 3C). The matrigel invasion assay also showed significant cell invasion inhibitions in the transfectants compared with the control from the BOY cell lines (35.625 ± 4.606, 24.000 ± 4.516, 182.000 ± 18.678, $P<0.0001$; Figure 3D). However, no significant difference was observed in the *miR-145* and *miR-133a* transfectants from T24 cell lines (173.875 ± 16.607, 140.125 ± 6.799, 167.000 ± 27.367; Figure 3D). We did not subject KK47 cell line to these experiments because it showed a focal growth and it was not suitable for the experiments.

Effect of FSCN1 knockdown on cell growth, invasion, and migration activity in BC cell lines

The expression levels of *FSCN1* mRNA were more than three-fold higher in BC cell lines than in the control (normal human bladder RNA). To examine the functional role of FSCN1, we performed loss of function studies using si-FSCN1-transfected T24 cell lines, which showed higher *FSCN1* mRNA expression levels compared with BOY (Figure 4A, upper). We did not subject KK47 cell line to these experiments because it showed a focal growth and it was not suitable for the experiments. FSCN1 protein expression was repressed by si-FSCN1 transfection (Figure 4A, lower). The XTT assay revealed significant cell-growth inhibition in the three si-FSCN1 transfectants in comparison with that in the si-control transfectant (% of cell viability; 69.9 ± 1.3, 88.7 ± 2.0, 58.0 ± 1.4, and 100.0 ± 1.3, respectively, $P<0.0001$; Figure 4B). The wound-healing assay also showed significant cell migration inhibitions in the si-FSCN1 transfectant compared with the counterparts (% of wound closure; 70.9 ± 2.5, 49.4 ± 2.5, 34.2 ± 2.6, and 100.0 ± 2.6, respectively, $P<0.0001$; Figure 4C). The matrigel invasion assay showed that the number of invading cell was significantly decreased in the si-FSCN1 transfectant compared with the counterparts (% of cell invasion; 39.0 ± 4.6, 35.1 ± 2.9, 18.3 ± 2.5, and 100.0 ± 3.9, respectively, $P<0.0001$; Figure 4D).

Immunohistochemistry of FSCN1 and *in situ* hybridisation of *miR-145* in clinical BC samples

To visualise FSCN1 expression and the related microRNA expression in a tumour lesion and surrounding normal tissues, we performed immunohistochemistry of FSCN1 and *in situ*

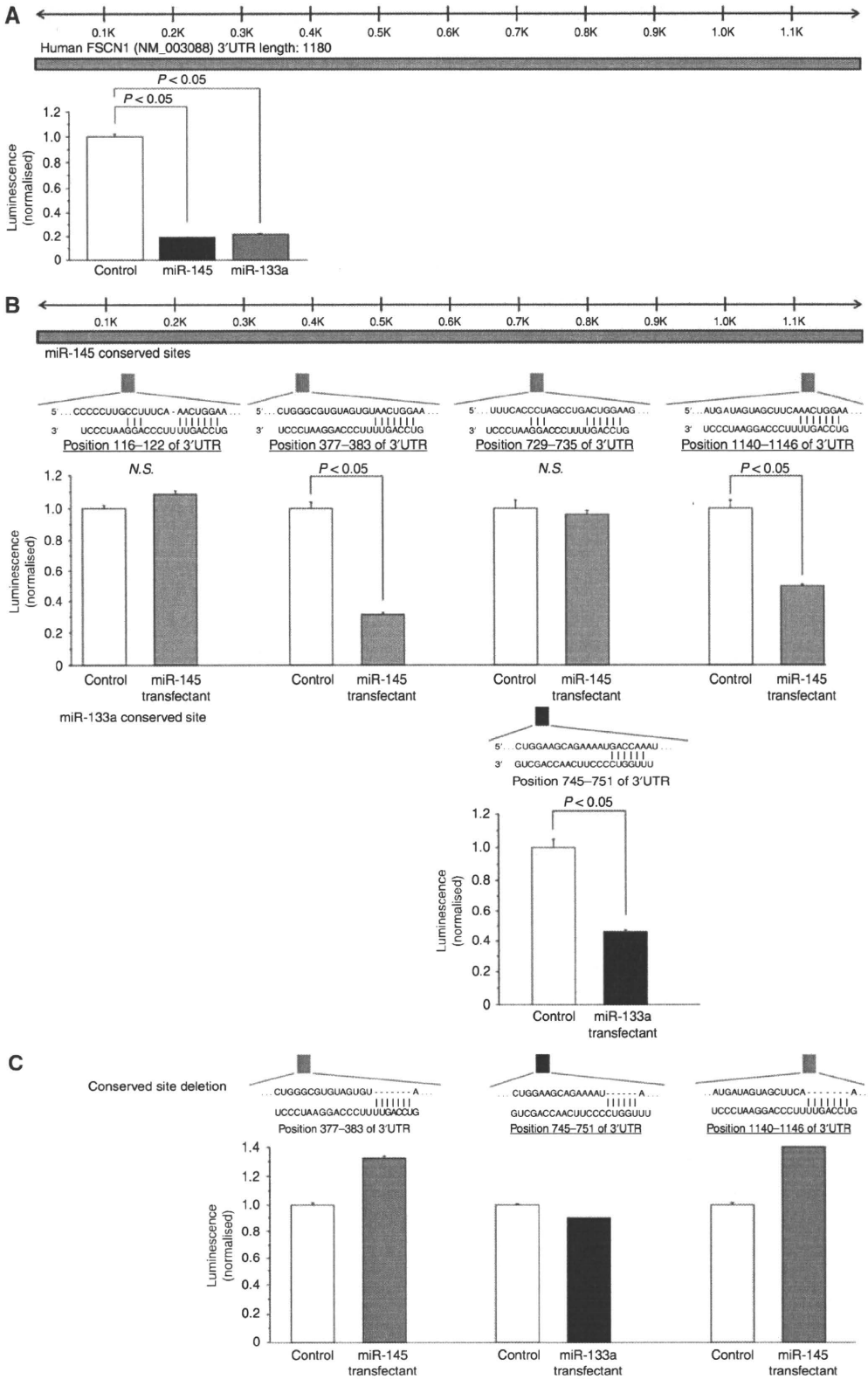

Figure 2 *miR-145*- and *miR-133a*-binding sites in *FSCN1* 3′-UTR. (**A**) A luciferase assay using the vector encoding full length of *FSCN1* 3′-UTR (position 51–1180). BOY cells were transfected with 5 ng vector and 10 nM microRNAs. The *Renilla* luciferase values were normalised by firefly-luciferase values. (**B**) Luciferase assays using the vectors encoding putative conserved target sites of *FSCN1* 3′-UTR identified with the TargetScan database: four conserved sites for *miR-145* and one site for *miR-133a*. (**C**) Luciferase assays using the mutated vectors in which the specific sites targeted by the microRNAs were deleted.

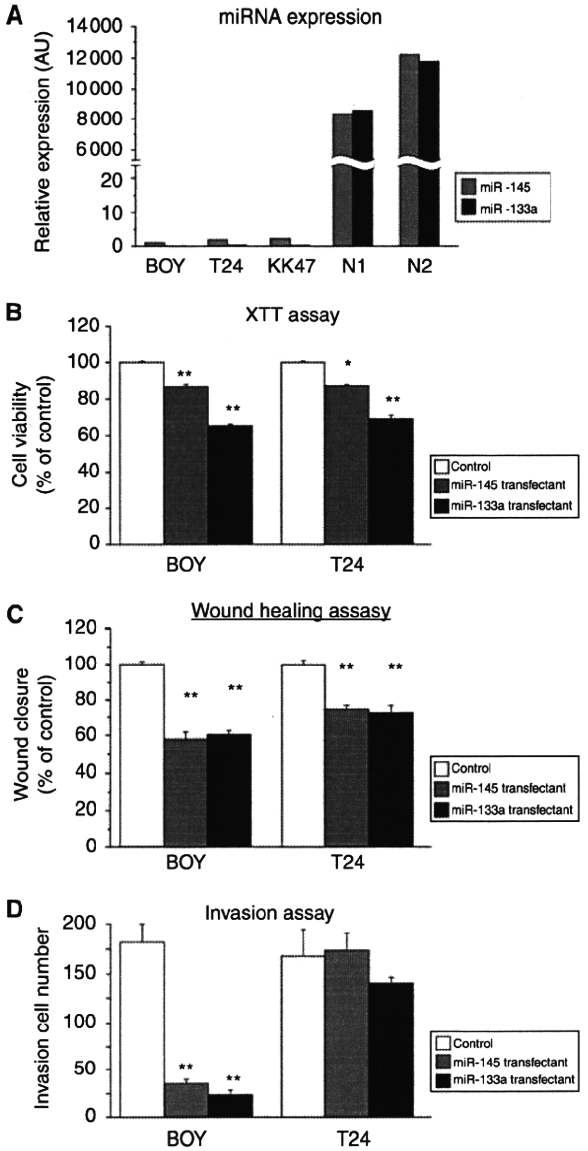

Figure 3 (**A**) *miR-145* and *miR-133a* expression in BC cell lines (BOY, T24, KK47) and normal human bladder mucosa (N1 and N2). (**B**–**D**) Effect of cell viabilities in *miR-145* and *miR-133a* transfectants: (**B**) cell growth determined by the XTT assay; (**C**) cell migration activity determined by the wound-healing assay; and (**D**) cell invasion activity determined by the matrigel invasion assay in BOY and T24 cell lines transfected with *miR-145* and *miR-133a*. *$P<0.005$, **$P<0.0001$.

hybridisation of *miR-145* in FFPE tissues (Figure 5). H&E staining showed a high-grade tumour lesion surrounded by smooth muscle layers (Figure 5A). Immunohistochemistry revealed that FSCN1 was markedly expressed in the tumour lesion, whereas no expression was observed in adjacent tissues including the smooth muscle layers (Figure 5B). In contrast, *miR-145* was faintly expressed in the tumour lesion with the strong expression in the smooth muscle layers (Figure 5C). The scramble-control probe showed no significant staining in either the tumour or the smooth muscle layers (Figure 5D). Figure 5E shows immunostaining of FSCN1 in a non-invasive BC (pTa) and an invasive BC with involvement of the muscularis (pT2). There was faint staining in the non-invasive BC, whereas there was strong staining of cytosol and nuclei in the invasive BC. The staining score of the invasive BC ($\geqslant$pT1) was significantly higher than that of the non-invasive BC (pTa) (1.62 ± 0.05 *vs* 1.33 ± 0.07, $P=0.0055$). We found no correlation between FSCN1 expression and clinico-pathological parameters except for tumour stage.

DISCUSSION

Earlier studies showed that *miR-145* and *miR-133a* are commonly down-regulated in several human cancers and that their transfection reduces cell proliferation of each cancer cell line (Bandrés *et al*, 2006; Sempere *et al*, 2007; Slaby *et al*, 2007; Szafranska *et al*, 2007; Ozen *et al*, 2008; Schepeler *et al*, 2008; Wang *et al*, 2008, 2009a, b; Wong *et al*, 2008a; Childs *et al*, 2009; Friedman *et al*, 2009; Liu *et al*, 2009; Takagi *et al*, 2009; Tong *et al*, 2009; Lin *et al*, 2009a). Consistent with earlier studies, we found significant cell-growth inhibitions in BC cell lines transfected with *miR-145* and *miR-133a* precursors. These results suggest that these microRNAs may have tumour suppressive functions through regulating oncogenic genes in human malignancies. Regarding BC, *miR-145* was listed in two of the three earlier studies investigating microRNA signatures in BC compared with normal control (Friedman *et al*, 2009; Lin *et al*, 2009a, b). Moreover, this study is the first to show that *miR-133a* is a down-regulated microRNA in BC. An earlier study showed that *miR-133a* is abundantly expressed in muscle cells, and it may have a part in regulating proliferation and differentiation (McCarthy and Esser, 2007). Regarding the target genes, there are only three earlier studies showing that *miR-145* directly binds to c-Myc (Sachdeva *et al*, 2009) and insulin receptor substrate-1 (Shi *et al*, 2007), which are associated with cell proliferation and that *miR-133a/b* directly binds to pyruvate kinase type M2 expression, which is a potent oncogene in solid cancers (Wong *et al*, 2008b). Down-regulation of these microRNAs may have a critical function in BC development. Our cell invasion assay showed that there were significant decreases of invading cell number in the *miR-145* and *miR133a* transfectants from BOY, but not from T24 BC cell lines. These results suggest that another pathway might be more crucial than FSCN1 for invasiveness in some BCs. To find the target genes, web-based software was used in the earlier studies. However, the many candidate microRNAs identified by the web-based software often make it more difficult for researchers to find the crucial target genes. In this study, we used an oligo-microarray to screen the candidates from gene expression profiles in *miR-145* transfectant and found a new target gene, FSCN1, which was subsequently validated by the luciferase reporter assay. Thus, gene expression profiles from specific microRNA transfectant may be a good strategy for finding candidate genes targeted by microRNA.

FSCN1 functions in two major forms of actin-based structures: cortical cell protrusions that mediate interactions between cells and the extra-cellular matrix (ECM), cell-to-cell interactions, and cell migration; and cytoplasmic microfilamentous bundles that contribute to cell architecture and intracellular movements (Kureishy *et al*, 2002). The fascin–actin interaction is affected by extra-cellular cues, and certain ECM components induce bundling of actin by FSCN1 (Hashimoto *et al*, 2005). It is plausible that the activation of fascin through ECM substrates contributes to tumour growth, migration, and invasion. In BC, FSCN1 over-expression has been noted in three different immunohistochemistry studies (Tong *et al*, 2005; Karasavvidou *et al*, 2008; Soukup *et al*, 2008). Our immnohistochemical study consistently showed that the expression levels of FSCN1 were correlated with advanced tumour stage. In addition, tumour viability was markedly decreased in FSCN1-knockdown BC cell lines. These results strongly suggest that this molecule may function as an oncogene. It may be deeply

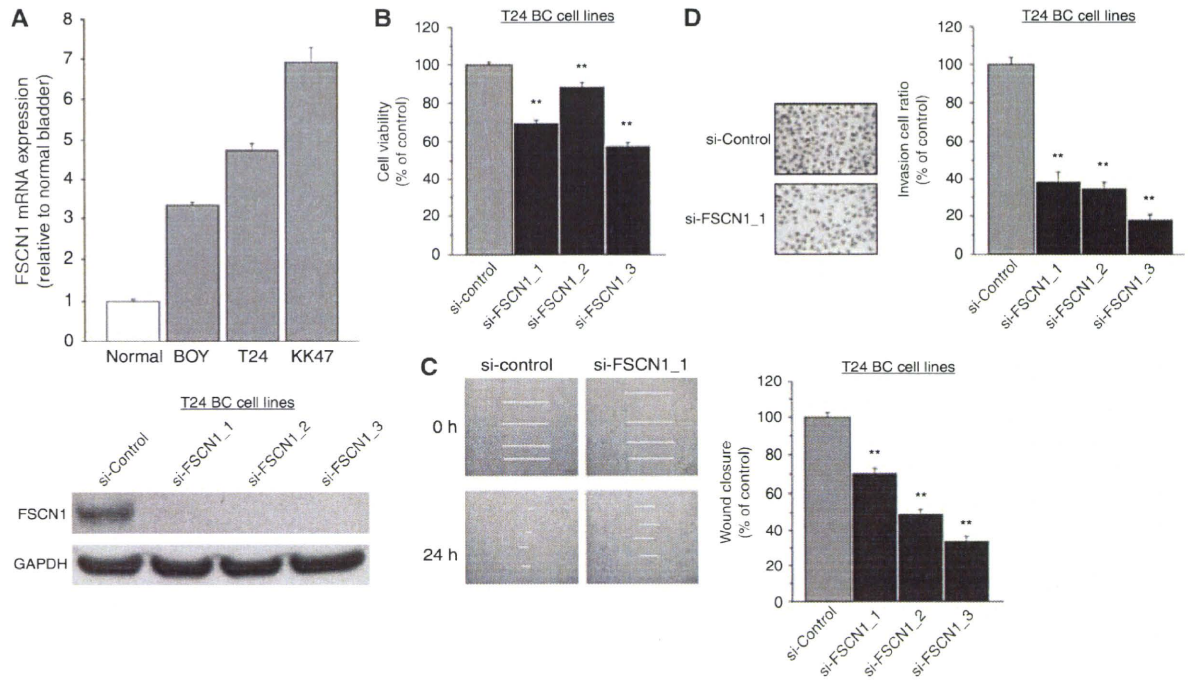

Figure 4 FSCN1-knockdown effect on BC cell viability by si-RNA: (**A**) upper, *FSCN1* mRNA expression in three BC cell lines (BOY, T24, KK47) by real-time RT–PCR; (**A**) lower, western blot revealed that FSCN1 protein was markedly decreased in three si-FSCN1 transfectants compared with the controls; (**B**) cell growth as revealed by the XTT assay; (**C**) cell migration activity by the wound-healing assay; and (**D**) cell invasion activity by the matrigel invasion assay in T24 cell lines transfected with si-FSCN1. si-FSCN1-transfected T24 cell lines exhibited a significant decrease in cell growth, migration, and invasion in comparison with the si-control transfectants. $^{**}P<0.0001$.

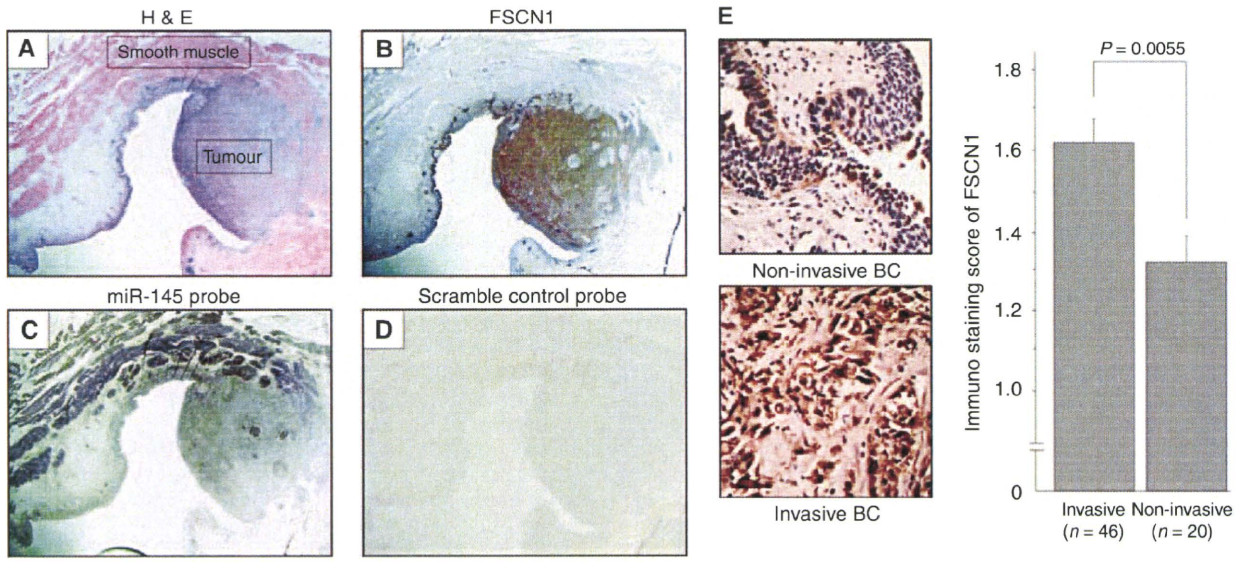

Figure 5 *In situ* hybridisation of *miR-145* and immunohistochemistry examination of FSCN1 in clinical BC specimens: (**A**) H&E staining, tumour, and surrounding smooth muscle; (**B**) immunohistochemical staining of FSCN1 showing strong expression in tumour lesion; (**C**) *in situ* hybridisation of *miR-145* showing faint expression in tumour lesion and strong expression in smooth muscle layer; (**D**) no staining by scramble-control probe; and (**E**) FSCN1 protein expression in invasive and non-invasive BC specimens. Low-grade bladder cancer without invasion (pTa) (upper panel, original magnification × 400). High-grade bladder cancer with involvement of the muscularis (pT2) (lower panel, original magnification × 400).

associated with BC invasiveness and might be a useful staging biomarker for clinical BC.

Regarding FSCN1 regulation, several studies have reported that the actin-binding activity of fascin is inhibited by phosphorylation of residue Ser-39 by protein kinase Cα (Adams *et al*, 1999); β-catenin/T cell factor signalling transactivates the FSCN1 promoter in human colon carcinoma cell lines (Vignjevic *et al*, 2007); and FSCN1 down-regulation is associated with a decrease in β-catenin and c-erbB-2 expression (Xie *et al*, 2005). However, to our knowledge, there has been no earlier study reporting the

interaction between FSCN1 expression and particular microRNAs. We earlier reported that *miR-145* and *miR-133a* expressions are significantly down-regulated in BC tissue compared with normal bladder epithelium (Ichimi *et al*, 2009). In this study, we showed that *miR-145* and *miR-133a* directly target FSCN1, resulting in decreased *FSCN1* mRNA and its protein levels both *in vitro* and in clinical specimens. The question of how FSCN1 becomes over-expressed is still open, but one possible mechanism is through regulation by microRNAs. Loss of *miR-145* and *miR-133a*, both of which are endogenous FSCN1 inhibitors, may promote aberrant expression of FSCN1 contributing to pathogenesis and progression of BC.

In summary, through our microRNA profiling in BC, we have found that FSCN1 might have an oncogenic function in BC and *miR-145* and *miR-133a* might function as tumour suppressors through direct repression of FSCN1 in BC. As viral vector-mediated microRNA transduction might be applicable *in vivo* (Yang *et al*, 2006), our findings raise the possibility that *miR-145* and *miR-133a* may have potential therapeutic value in BC patients. In addition, FSCN1 may be a potential target for gene therapy of BC. As down-regulation of *miR-145* and *miR-133a* and over-expression of FSCN1 were commonly identified in various human malignancies, our findings may be crucial events in the development throughout human malignancies.

ACKNOWLEDGEMENTS

We thank Ms M Miyazaki for her excellent laboratory assistance.

REFERENCES

Adams JC, Clelland JD, Collett GD, Matsumura F, Yamashiro S, Zhang L (1999) Cell–matrix adhesions differentially regulate fascin phosphorylation. *Mol Biol Cell* **10:** 4177–4190

Bandrés E, Cubedo E, Agirre X, Malumbres R, Zárate R, Ramirez N, Abajo A, Navarro A, Moreno I, Monzó M, García-Foncillas J (2006) Identification by real-time PCR of 13 mature microRNAs differentially expressed in colorectal cancer and non-tumoral tissues. *Mol Cancer* **5:** 29

Childs G, Fazzari M, Kung G, Kawachi N, Brandwein-Gensler M, McLemore M, Chen Q, Burk RD, Smith RV, Prystowsky MB, Belbin TJ, Schlecht NF (2009) Low-level expression of microRNAs let-7d and miR-205 are prognostic markers of head and neck squamous cell carcinoma. *Am J Pathol* **174:** 736–745

Darnel AD, Behmoaram E, Vollmer RT, Corcos J, Bijian K, Sircar K, Su J, Jiao J, Alaoui-Jamali MA, Bismar TA (2009) Fascin regulates prostate cancer cell invasion and is associated with metastasis and biochemical failure in prostate cancer. *Clin Cancer Res* **15:** 1376–1383

Friedman JM, Liang G, Liu CC, Wolff EM, Tsai YC, Ye W, Zhou X, Jones PA (2009) The putative tumor suppressor microRNA-101 modulates the cancer epigenome by repressing the polycomb group protein EZH2. *Cancer Res* **69:** 2623–2629

Goncharuk VN, Ross JS, Carlson JA (2002) Actin-binding protein fascin expression in skin neoplasia. *J Cutan Pathol* **29:** 430–438

Grothey A, Hashizume R, Ji H, Tubb BE, Patrick Jr CW, Yu D, Mooney EE, McCrea PD (2000) C-erbB-2/HER-2 upregulates fascin, an actin-bundling protein associated with cell motility, in human breast cancer cell lines. *Oncogene* **19:** 4864–4875

Hashimoto Y, Skacel M, Adams JC (2005) Roles of fascin in human carcinoma motility and signaling: prospects for a novel biomarker? *Int J Biochem Cell Biol* **37:** 1787–1804

Ichimi T, Enokida H, Okuno Y, Kunimoto R, Chiyomaru T, Kawamoto K, Kawahara K, Toki K, Kawakami K, Nishiyama K, Tsujimoto G, Nakagawa M, Seki N (2009) Identification of novel microRNA targets based on microRNA signatures in bladder cancer. *Int J Cancer* **125:** 345–352

Jawhari AU, Buda A, Jenkins M, Shehzad K, Sarraf C, Noda M, Farthing MJ, Pignatelli M, Adams JC (2003) Fascin, an actin-bundling protein, modulates colonic epithelial cell invasiveness and differentiation *in vitro*. *Am J Pathol* **162:** 69–80

Jemal A, Siegel R, Ward E, Hao Y, Xu J, Murray T, Thun MJ (2008) Cancer statistics, 2008. *CA Cancer J Clin* **58:** 71–96

Karasavvidou F, Barbanis S, Pappa D, Moutzouris G, Tzortzis V, Melekos MD, Koukoulis G (2008) Fascin determination in urothelial carcinomas of the urinary bladder: a marker of invasiveness. *Arch Pathol Lab Med* **132:** 1912–1915

Kloosterman WP, Wienholds E, de Bruijn E, Kauppinen S, Plasterk RH (2006) *In situ* detection of miRNAs in animal embryos using LNA-modified oligonucleotide probes. *Nat Methods* **3:** 27–29

Kureishy N, Sapountzi V, Prag S, Anilkumar N, Adams JC (2002) Fascins, and their roles in cell structure and function. *Bioessays* **24:** 350–361

Kwak C, Ku JH, Park JY, Lee E, Lee SE, Lee C (2004) Initial tumor stage and grade as a predictive factor for recurrence in patients with stage T1 grade 3 bladder cancer. *J Urol* **171:** 149–152

Lagos-Quintana M, Rauhut R, Lendeckel W, Tuschl T (2001) Identification of novel genes coding for small expressed RNAs. *Science* **294:** 853–858

Lin CK, Chao TK, Yu CP, Yu MH, Jin JS (2009b) The expression of six biomarkers in the four most common ovarian cancers: correlation with clinicopathological parameters. *APMIS* **117:** 162–175

Lin T, Dong W, Huang J, Pan Q, Fan X, Zhang C, Huang L (2009a) MicroRNA-143 as a tumor suppressor for bladder cancer. *J Urol* **181:** 1372–1380

Liu X, Sempere LF, Galimberti F, Freemantle SJ, Black C, Dragnev KH, Ma Y, Fiering S, Memoli V, Li H, DiRenzo J, Korc M, Cole CN, Bak M, Kauppinen S, Dmitrovsky E (2009) Uncovering growth-suppressive MicroRNAs in lung cancer. *Clin Cancer Res* **15:** 1177–1183

Maitra A, Adsay NV, Argani P, Iacobuzio-Donahue C, De Marzo A, Cameron JL, Yeo CJ, Hruban RH (2003) Multicomponent analysis of the pancreatic adenocarcinoma progression model using a pancreatic intraepithelial neoplasia tissue microarray. *Mod Pathol* **16:** 902–912

McCarthy JJ, Esser KA (2007) MicroRNA-1 and microRNA-133a expression are decreased during skeletal muscle hypertrophy. *J Appl Physiol* **102:** 306–313

Ozen M, Creighton CJ, Ozdemir M, Ittmann M (2008) Widespread deregulation of microRNA expression in human prostate cancer. *Oncogene* **27:** 1788–1793

Parkin DM, Bray F, Ferlay J, Pisani P (2005) Global cancer statistics, 2002. *CA Cancer J Clin* **55:** 74–108

Pelosi G, Pastorino U, Pasini F, Maissoneuve P, Fraggetta F, Iannucci A, Sonzogni A, De Manzoni G, Terzi A, Durante E, Bresaola E, Pezzella F, Viale G (2003) Independent prognostic value of fascin immunoreactivity in stage I non-small cell lung cancer. *Br J Cancer* **88:** 537–547

Qiu D, Katanoda K, Marugame T, Sobue T (2009) A joinpoint regression analysis of long-term trends in cancer mortality in Japan (1958–2004). *Int J Cancer* **124:** 443–448

Ropponen KM, Eskelinen MJ, Lipponen PK, Alhava EM, Kosma VM (1999) Reduced expression of á catenin is associated with poor prognosis in colorectal carcinoma. *J Clin Pathol* **52:** 10–16

Sachdeva M, Zhu S, Wu F, Wu H, Walia V, Kumar S, Elble R, Watabe K, Mo YY (2009) p53 represses c-Myc through induction of the tumor suppressor miR-145. *Proc Natl Acad Sci USA* **106:** 3207–3212

Schepeler T, Reinert JT, Ostenfeld MS, Christensen LL, Silahtaroglu AN, Dyrskjøt L, Wiuf C, Sørensen FJ, Kruhøffer M, Laurberg S, Kauppinen S, Ørntoft TF, Andersen CL (2008) Diagnostic and prognostic microRNAs in stage II colon cancer. *Cancer Res* **68:** 6416–6424

Schickel R, Boyerinas B, Park SM, Peter ME (2008) MicroRNAs: key players in the immune system, differentiation, tumorigenesis and cell death. *Oncogene* **27:** 5959–5974

Sempere LF, Christensen M, Silahtaroglu A, Bak M, Heath CV, Schwartz G, Wells W, Kauppinen S, Cole CN (2007) Altered microRNA expression confined to specific epithelial cell subpopulations in breast cancer. *Cancer Res* **67:** 11612–11620

Shi B, Sepp-Lorenzino L, Prisco M, Linsley P, deAngelis T, Baserga R (2007) Micro RNA 145 targets the insulin receptor substrate-1 and inhibits the growth of colon cancer cells. *J Biol Chem* **282:** 32582–32590

Slaby O, Svoboda M, Fabian P, Smerdova T, Knoflickova D, Bednarikova M, Nenutil R, Vyzula R (2007) Altered expression of miR-21, miR-31, miR-143 and miR-145 is related to clinicopathologic features of colorectal cancer. *Oncology* **72:** 397–402

Sobin LH, Wittekind C (2002) *TNM Classification of Malignant Tumours, 6th edn. International Union Against Cancer (UICC).* New York: Wiley-Liss. 199–202

Soukup V, Babjuk M, Dusková J, Pesl M, Szakáczová M, Zámecník L (2008) Does the expression of fascin-1 and tumor subclassification help to assess the risk of recurrence and progression in t1 urothelial urinary bladder carcinoma? *Urol Int* **80:** 413–418

Sugimoto T, Seki N, Shimizu S, Kikkawa N, Tsukada J, Shimada H, Sasaki K, Hanazawa T, Okamoto Y, Hata A (2009) The galanin signaling cascade is a candidate pathway regulating oncogenesis in human squamous cell carcinoma. *Genes Chromosomes Cancer* **48:** 132–142

Szafranska AE, Davison TS, John J, Cannon T, Sipos B, Maghnouj A, Labourier E, Hahn SA (2007) MicroRNA expression alterations are linked to tumorigenesis and non-neoplastic processes in pancreatic ductal adenocarcinoma. *Oncogene* **26:** 4442–4452

Takagi T, Iio A, Nakagawa Y, Naoe T, Tanigawa N, Akao Y (2009) Decreased expression of microRNA-143 and -145 in human gastric cancers. *Oncology* **77:** 12–21

Tong AW, Fulgham P, Jay C, Chen P, Khalil I, Liu S, Senzer N, Eklund AC, Han J, Nemunaitis J (2009) MicroRNA profile analysis of human prostate cancers. *Cancer Gene Ther* **16:** 206–216

Tong GX, Yee H, Chiriboga L, Hernandez O, Waisman J (2005) Fascin-1 expression in papillary and invasive urothelial carcinomas of the urinary bladder. *Hum Pathol* **36:** 741–766

van Rhijn BW, van der Poel HG, van der Kwast TH (2005) Urine markers for bladder cancer surveillance: a systematic review. *Eur Urol* **47:** 736–748

Vignjevic D, Kojima S, Aratyn Y, Danciu O, Svitkina T, Borisy GG (2006) Role of fascin in filopodial protrusion. *J Cell Biol* **174:** 863–875

Vignjevic D, Schoumacher M, Gavert N, Janssen KP, Jih G, Laé M, Louvard D, Ben-Ze'ev A, Robine S (2007) Fascin, a novel target of beta-catenin-TCF signaling, is expressed at the invasive front of human colon cancer. *Cancer Res* **67:** 6844–6853

Wang CJ, Zhou ZG, Wang L, Yang L, Zhou B, Gu J, Chen HY, Sun XF (2009b) Clinicopathological significance of microRNA-31, -143 and -145 expression in colorectal cancer. *Dis Markers* **26:** 27–34

Wang S, Bian C, Yang Z, Bo Y, Li J, Zeng L, Zhou H, Zhao RC (2009a) miR-145 inhibits breast cancer cell growth through RTKN. *Int J Oncol* **34:** 1461–1466

Wang X, Tang S, Le SY, Lu R, Rader JS, Meyers C, Zheng ZM (2008) Aberrant expression of oncogenic and tumor-suppressive microRNAs in cervical cancer is required for cancer cell growth. *PLoS One* **3:** e2557

Wong TS, Liu XB, Chung-Wai Ho A, Po-Wing Yuen A, Wai-Man Ng R, Ignace Wei W (2008a) Identification of pyruvate kinase type M2 as potential oncoprotein in squamous cell carcinoma of tongue through microRNA profiling. *Int J Cancer* **123:** 251–257

Wong TS, Liu XB, Wong BY, Ng RW, Yuen AP, Wei WI (2008b) Mature miR-184 as potential oncogenic microRNA of squamous cell carcinoma of tongue. *Clin Cancer Res* **14:** 2588–2592

Xie JJ, Xu LY, Zhang HH, Cai WJ, Mai RQ, Xie YM, Yang ZM, Niu YD, Shen ZY, Li EM (2005) Role of fascin in the proliferation and invasiveness of esophageal carcinoma cells. *Biochem Biophys Res Commun* **337:** 355–362

Yang L, Bailey L, Baltimore D, Wang P (2006) Targeting lentiviral vectors to specific cell types *in vivo*. *Proc Natl Acad Sci USA* **103:** 11479–11484

Zhang H, Xu L, Xiao D, Xie J, Zeng H, Cai W, Niu Y, Yang Z, Shen Z, Li E (2006) Fascin is a potential biomarker for early-stage oesophageal squamous cell carcinoma. *J Clin Pathol* **59:** 958–964

CpG hypermethylation of *human four-and-a-half LIM domains 1* contributes to migration and invasion activity of human bladder cancer

MITSUGI MATSUMOTO[1], KAZUMORI KAWAKAMI[1], HIDEKI ENOKIDA[1], KAZUKI TOKI[1], RYOICHIRO MATSUDA[1], TAKESHI CHIYOMARU[1], KENRYU NISHIYAMA[1], KAZUYA KAWAHARA[2], NAOHIKO SEKI[3] and MASAYUKI NAKAGAWA[1]

[1]Department of Urology, Graduate School of Medical and Dental Sciences, Kagoshima University; [2]Kawahara Nephro-urology Clinic, Kagoshima; [3]Department of Functional Genomics, Graduate School of Medicine, Chiba University, Chiba, Japan

DOI: 10.3892/ijmm_xxxxxxxx

Abstract. We previously reported a simple technique that combines microarray data from clinical bladder cancer (BC) specimens with those from a BC cell line (BOY) treated with a pharmacologic demethylating agent (5-aza-dC). We focused on the *human four-and-a-half LIM domains 1 (FHL1)* gene which was selected on the basis of previous microarray data analysis. Because LIM domains provide protein-protein binding interfaces, *FHL* genes play an important role in cellular events, such as focal adhesion and differentiation, by interacting with the target protein as either a repressor or activator. We hypothesized that inactivation of the *FHL1* gene through CpG methylation contributes to cell viability including migration and invasion activity of human BC. After 5-aza-dC treatment, the expression levels of *FHL1* mRNA transcript markedly increased in all cell lines tested, as shown by real-time reverse transcription-polymerase chain reaction (RT-PCR). The methylation index of *FHL1* in our samples was significantly higher in 70 BC specimens than in 10 normal bladder epithelium (NBE) specimens (63.9±25.5 and 0.3±0.2, respectively; p=0.0066). Conversely, *FHL1* mRNA expression was significantly lower in the BC specimens than in the NBE ones (0.331±0.12 and 2.498±0.61, respectively; p=0.0011). In addition, significant inhibitions of wound healing (45.78±6.2, and 100±0, respectively; p=0.009) and of cell invasion (18.5±2.3 and 95.2±2.4, respectively; p=0.02) were observed in stable *FHL1*-transfected cells than in the control BC cells. In conclusion, we found that the mechanism of *FHL1* down-regulation in BC is through CpG hypermethylation of the promoter region. *FHL1* gene inactivation by CpG hypermethylation may thus contribute to migration and invasion activity of BC.

Correspondence to: Dr Kazumori Kawakami, Department of Urology, Graduate School of Medical and Dental Sciences, Kagoshima University, 8-35-1 Sakuragaoka, Kagoshima 890-8520, Japan
E-mail: kkawakam@m.kufm.kagoshima-u.ac.jp

Key words: bladder cancer, microarray, *FHL1*, methylation

Introduction

Bladder cancer (BC), one of the five most common malignancies in the US, is the second most common tumor of the genitourinary tract and the second most common cause of death in patients with urinary tract malignancies (1). As in other human cancers, loss of function of tumor suppressor genes and activation of oncogenes are two major alterations that promote BC initiation and progression (2). Our laboratory developed a simple technique that combines microarray data from clinical BC specimens with those from a BC cell line (BOY) treated with a pharmacologic demethylating agent (5-aza-dC) (3,4). As described in a previous report (4), we used it to identify the methylated gene profile in human BC; this profile contains 24 methylated genes. Among these genes, we focused on the *human four-and-a-half LIM domains 1 (FHL1)* gene, one of the down-regulated genes in the gene expression profile of human BC (3).

The *FHL* family genes are characterized by LIM domains. Because LIM domains provide protein-protein binding interfaces, *FHL* genes play an important role in cellular events, such as focal adhesion and differentiation, by interacting with the target protein as either a repressor or activator (5-7). The molecules associated with intercellular adhesion are possibly inhibited during tumor progression (8). The expression of the *FHL1* gene, located at human chromosome Xq26, is down-regulated in various types of malignancies including lung, prostate, breast, ovarian, colon, and thyroid cancer, brain tumors, renal cancer, liver cancer, melanoma, and gastric cancer (9-13).

Gene function can be altered by epigenetic mechanisms. Silencing of tumor suppressor genes by hypermethylation of CpG islands within the promoter and/or 5'-regions is a common feature of human cancer and is often associated

with partial or complete transcriptional blocking. Many tumor suppressor genes silenced by DNA methylation have been identified in various types of cancer including BC (14,15). However, little is known about the status of *FHL1* promoter methylation and the functional role of *FHL1* in BC. We hypothesized that inactivation of the *FHL1* gene through CpG methylation contributes to cell viability including migration and invasion activity of human BC. To test this hypothesis, we investigated the mRNA expression levels in BC cell lines and human BC tissue. Methylation status was determined by real-time quantitative methylation-specific polymerase chain reaction (PCR) in BC specimens. In addition, we established stable *FHL1*-transfected cells and compared their proliferation, migration, and invasion activities with those of the control BC cell line.

Materials and methods

Clinical samples. A total of 70 pathologically proven BC specimens were obtained from BC patients who underwent TUR-Bt or radical cystectomy at Kagoshima University Hospital and affiliated hospitals between 2003 and 2008. Also obtained were ten normal bladder epithelium (NBE) specimens from patients without BC. The background and clinicopathological characteristics of the patients are summarized in Table I. Each tumor was staged and graded in accordance with the tumor-node-metastasis (TNM) staging system (16). The study was approved by the Institutional Review Board of our institution; written prior informed consent was obtained from all patients for use of their specimens and clinical and pathological data.

Cell culture and 5-Aza-dC treatment. The human BC cell lines (T24, UMUC and BOY) were maintained in MEM mixed with 10% FBS and 1% penicillin/streptomycin in a humidified atmosphere of 5% CO_2 and 95% air at 37°C. To screen for epigenetic alterations of gene methylation, these cell lines were treated with a DNA methyltransferase inhibitor, 5-aza-dC (Sigma-Aldrich, St. Louis, MO). Cultured cells were harvested after seven days of exposure to 10 μM of 5-aza-dC, and total RNA was extracted from the cell lines before and after drug treatment.

Nucleic acid extraction. Genomic DNA was extracted from the BC and NBE specimens with a QIAamp tissue kit (Qiagen, Valencia, CA) after microdissection of 10-μm-thick paraffin-embedded sections. It was precipitated with ethanol. Total RNA was extracted from the clinical specimens using Isogen (Nippon Gene, Tokyo, Japan), following the manufacturer's protocol. Total RNA was extracted from the human BC cell lines with a QIAamp DNA/RNA Mini kit (Qiagen) according to the manufacturer's instructions. The concentration of nucleic acid was determined with a spectrophotometer, and the integrity was checked by gel electrophoresis.

cDNA preparation and real-time quantitative RT-PCR. First strand cDNA with 1 μg of total RNA was synthesized using random primers of high capacity cDNA reverse transcription kit (Applied Biosystems). Premium total RNA from normal human bladder (Clontech, Palo Alto, CA) was used as a normal bladder control. Gene-specific PCR products were continuously measured using an Applied Biosystems 7300 real-time PCR system, following the manufacturer's protocol. The first PCR step was a 10 min hold at 95°C followed by 45 cycles and the 45 cycles of a 15 sec denaturation step at 95°C and a 1 min annealing/extension step at 60°C. All reactions were performed in triplicate, and a negative control lacking cDNA was included. TaqMan® probes and primers for *FHL1* (P/N: Hs00793641_g1, Applied Biosystems) and *Glucuronidase ß* (*GUSB*) (P/N: Hs99999908_m1, Applied Biosystems) were the assay-on-demand gene expression products. The expression of *FHL1* mRNA was normalized to the amount of *GUSB* in the same cDNA using the standard curve method provided by the manufacturer.

Table I. Patient characteristics.

Bladder cancer (BC)		
Total number	70	
Median age (range)	74	(49-100) yrs
Gender		
Male	46	
Female	24	
Stage		
Tis	1	
Superficial (pTa)	16	
Invasive (≥pT1)	53	
Grade		
G1	5	
G2	40	
G3	22	
Unknown	3	
Operation		
Cystectomy	8	
TUR-Bt	62	
Recurrence		
Recurrence	36	
Recurrence (-)	29	
Unknown	5	
Follow-up period (range)	513	(13-1440) days
Normal bladder epithelium (NBE)		
Total number	10	
Median age (range)	66	(58-76) yrs
Gender		
Male	8	
Female	2	

Real-time quantitative methylation-specific PCR. For TaqMan quantitative methylation-specific PCR (QMSP), the fluorescent probe and primer sets were designed to hybridize to the amplified region of DNA (Fig. 1). Myogenic differentiation-1 (MYOD1) primer sequences were used as an internal control (4). The first PCR was amplified with universal primers (Pan-S; GGTTTGTTATTAAGGGGAGG and Pan-AS;

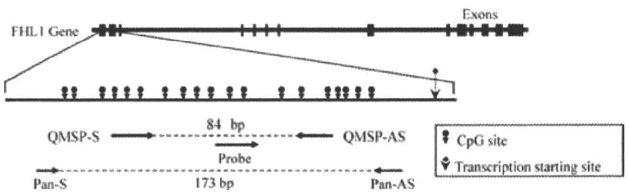

Figure 1. Schematic representation of location of CpG sites and primers designed within functional promoter of *FHL1* gene. First, universal PCR was performed with universal primers Pan-sense (S) and Pan-antisense (AS), which do not carry any CpG sites. Quantitative MSP was done using primer sets MSP-S and MSP-AS, and USP-S and USP-AS, respectively, and the universal PCR product was used as a template. For TaqMan QMSP, the fluorescent probe and primer sets were designed to hybridize to the amplified DNA region.

ACAAAAACAACCAAATAAAAATAAC) using 3 μl of bisulfite-treated DNA in a total volume of 20 μl. The first PCR step was 10 min hold at 95°C followed by 45 cycles of a 1 min denaturation step at 95°C, a 1 min annealing step at 48°C, and a 1-min extension step at 72°C. A second round of nested QMSP was then carried out using 1 μl of the first PCR product with the same PCR conditions described above except for the annealing temperature (59°C). The PCR cycle was programmed up to 45 cycles, and all reactions were performed in duplicate. The primers and probe sequences were QMSP primers, 5'-GTCGTTGTAAGTTATCGGGTTTC-3' (sense), 5'-CTACGCACTCCCTAAAAACG-3' (antisense), and 5'-A GGTCGAAACGGCGTGG-3' (probe). Serial dilutions of CpGenome universal methylated DNA (Millipore, Tokyo, Japan) were used to construct a calibration curve. The methylation index was defined as the quantity of fluorescence intensity derived from *FHL1* promoter amplification divided by the fluorescence intensity from MYOD1 amplification, multiplied by 1000.

Immunoblotting. Total protein lysate was prepared with detergent lysis buffer in the presence of a protease inhibitor. Twenty micrograms of protein lysate was separated by NuPAGE on 4-12% bis-tris gel (Invitrogen, Tokyo, Japan) and transferred into a PVDF membrane. Immunoblotting was done with diluted (1/200) polyclonal FHL1 antibody (10991-1-AP, Protein Tech Group, Chicago, IL). After being washed, the membrane was incubated with goat anti-rabbit IgG horseradish peroxidase conjugate (Bio-Rad, Hercules, CA). Specific complexes were visualized with an echochemiluminescence detection system (GE Healthcare Bio-Sciences, Buckinghamshire, UK).

Construction of FHL1 expression vectors and transfection to BOY cells. The *FHL1* vector was constructed by inserting full-length *FHL1* cDNA into the Sse83871 and *Hin*dIII restriction site of the pBApo-CMV Neo^{TM} vector (Takara Bio, Otsu, Japan). The *FHL1* and non-targeting (control) vector were transfected into BOY cells by calcium phosphate co-precipitation. The cells were then split and grown in selective medium with 1000 μg/ml of G418. After 2 weeks, G418-resistant colonies were chosen and expanded in medium containing 100 μg/ml of G418.

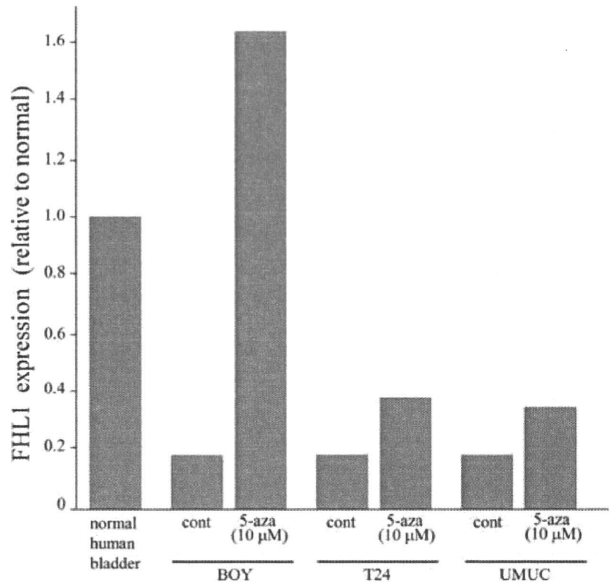

Figure 2. *FHL1* mRNA expression in BC cells before and after treatment with 5-aza-dC. Quantitative real-time RT-PCR demonstrated that mRNA transcript of *FHL1* gene was markedly increased after 5-aza-dC treatment especially in BOY cells. PCR conditions and primer sequences are described in Materials and methods section.

XTT assays. *FHL1*-transfected, control, and wild-type BOY cells were transferred to 96-well plates ($3x10^3$ cells/well) and incubated for 72 h. A 50 μl solution of XTT (0.3 mg/ml) containing 1.25 μM of PMS was then added to each well. The absorbance at 492 nm was measured after another 4 h of incubation at 37°C.

Wound healing assay. *FHL1*-transfected, control, and wild-type BOY cells were initially seeded uniformly onto 60 mm culture plates. An artificial 'wound' was carefully created at 0 h by using a P-20 pipette tip to scratch the subconfluent cell monolayer. Microphotographs were taken at 0 and 12 h. Quantitative analysis of the percentage of wound healing was calculated using the distance across the wound (n=5) at 0 and 12 h, divided by the distance measured at 0 h for each cell line. The experiment was repeated twice in sets of two, independently.

Invasion assay. A cell invasion assay was carried out using modified Boyden chambers consisting of Transwell-precoated Matrigel membrane filter inserts with 8 μm pores in 24-well tissue culture plates (BD Biosciences, Bedford, MA). Two days after transfection with *FLH-1*, $5x10^4$ BOY cells were placed in the top of the chamber in serum-free DMEM, and the bottom chamber was filled with DMEM containing 10% FBS as a chemoattractant. After 22 h of incubation in 5% CO_2 humidity at 37°C, non-invading cells were removed from the upper filter surfaces, and the filters were washed, fixed, and stained using a Diff-Quick kit (Sysmex, Kobe, Japan). Four randomly selected fields, magnification x200, were photographed, and the number of invading cells in each was counted. The experiment was repeated twice in sets of two, independently.

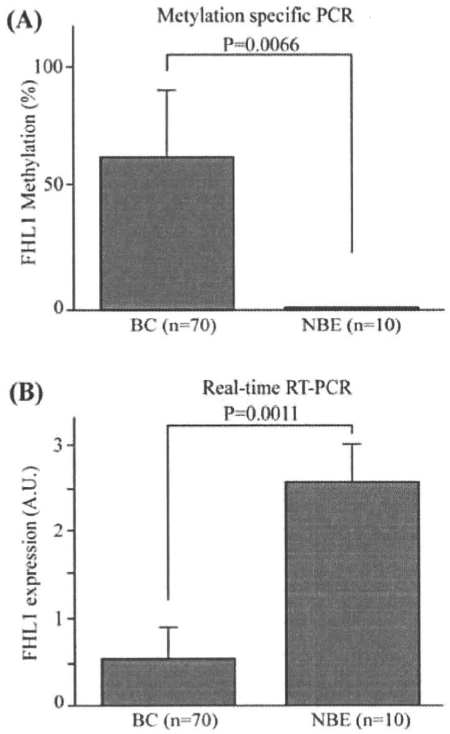

Figure 3. *FHL1* methylation index and mRNA expression of BC and NBE specimens. (A) *FHL1* methylation index was significantly higher for BC (p=0.0066). Methylation index was defined as described in Materials and methods section. (B) *FHL1* mRNA expression was significantly lower in BC (p=0.0011).

Statistical analysis. The relationship between two groups and the numerical value obtained by real-time RT-PCR was analyzed using the Mann-Whitney U test. The relationship between the BC and NBE specimens with *FHL1* methylation status was carried out using the χ^2 test. The analysis software was Expert StatView (version 4, SAS Institute Inc., Cary, NC), and the differences of $p<0.05$ were considered statistically significant.

Results

Validation of altered FHL1 mRNA expression in BC cell lines before and after 5-aza-dC treatment. The three BC cell lines (T24, UMUC and BOY) were subjected to real-time RT-PCR experiments to evaluate the mRNA expression levels of *FHL1* (Fig. 2). Before 5-aza-dC treatment, the *FHL1* mRNA expression levels in the BC cell lines were down-regulated and were lower than those of the normal human bladder. After 5-aza-dC treatment, the *FHL1* mRNA expression was up-regulated in the BC cell lines, and it was markedly higher in the BOY cells, which had been subjected to cDNA microarray analysis for obtaining the methylated gene profile in BC. Hence, the pattern of *FHL1* mRNA expression by 5-aza-dC treatment was validated by both real-time RT-PCR and cDNA microarray analysis (4).

Methylation status of FHL1 gene promoter and FHL1 mRNA expression in human BC specimens. We used QMSP and real-time quantitative RT-PCR to evaluate the methylation status of the *FHL1* promoter region and the expression levels of *FHL1* mRNA. The methylation index of the BC specimens was significantly higher than that of the NBE ones (63.9±25.5 and 0.3±0.2, respectively; p=0.0066) (Fig. 3A). In contrast, the expression level of *FHL1* mRNA in the BC specimens was significantly lower than that in the NBE ones (0.331±0.12 and 2.498±0.61, respectively; p=0.0008) (Fig. 3B). These results indicate that *FHL1 mRNA* expression might be down-regulated by methylation of the *FHL1* promoter region. We found no relationship between the clinicopathological parameters and the *FHL1* methylation index or mRNA expression (data not shown).

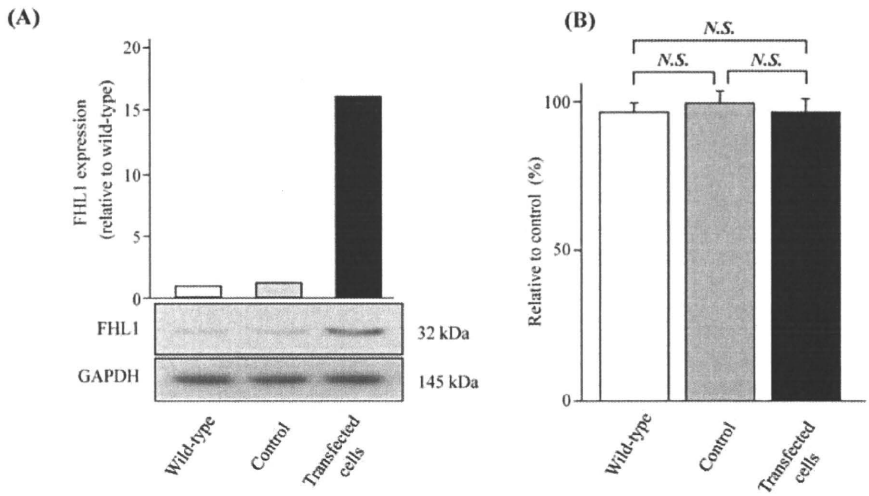

Figure 4. Effect of *FHL1* transfection on cell growth. (A) Expression level of *FHL1* mRNA was more than 16-fold higher in *FHL1*-transfected cells than in the control and the wild-type cells (upper; real-time RT-PCR). Western blot analysis revealed high expression levels of FHL1 in *FHL1*-transfected cells compared to control and wild-type cells (lower). (B) Cell growth determined by XTT assay. There was no significant difference in anchorage-dependent cell growth for *FHL1*-transfected, control, and wild-type BOY cells.

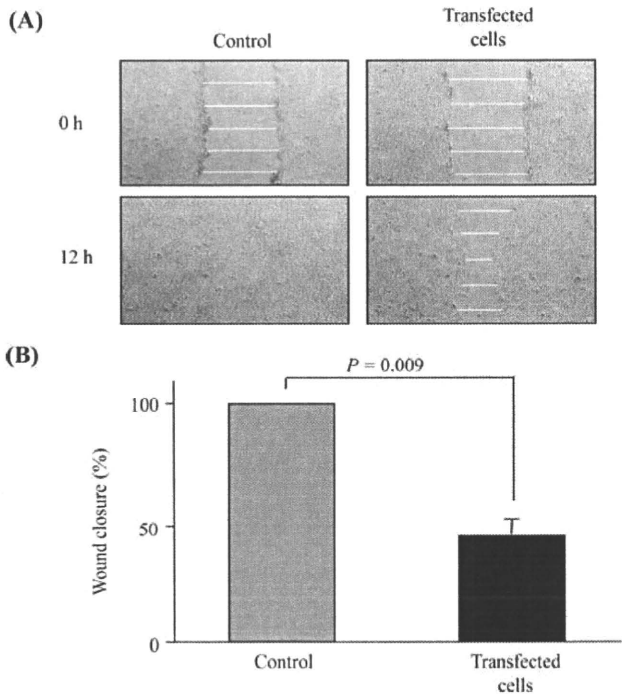

Figure 5. Effect of *FHL1* transfection on cell migration. (A) Representative photographs of cell migration activity from the wound healing assay. Wound was completely closed at 12 h after scratching in control cells whereas it was still open in *FHL1*-transfected cells. (B) Percentage of wound closure corres-ponding to distance between wound edges at 12 h in five randomly chosen regions (mean ± SD) relative to distance at time 0 h for each cell.

Identification of FHL1 expression in transfected cells and effect of FHL1 overexpression on cell proliferation. Because we found an extremely low expression of *FHL1* mRNA and a marked retrieval of the gene expression after 5-aza-dC treatment in the BOY cells (Fig. 2), we established stable *FHL1*-transfected BOY cells. The expression level of *FHL1* mRNA was more than 16-fold higher in the transfected cells than in the control and wild-type cells (Fig. 4A, upper). Western blot analysis demonstrated that the expression levels of the *FHL1*-transfected cells were high (Fig. 4A, lower). For gain-of-function experiments, we first performed XTT cell growth assay using *FHL1*-transfected, control, and wild-type BOY cells. We found no significant difference in anchorage-dependent cell growth among the three groups from three independent assays (Fig. 4B).

Effect of FHL1 transfection on cellular migration and invasion. To evaluate cellular migration, we performed wound healing assay using *FHL1*-transfected and control BOY cells. As shown in Fig. 5A, the cell migration ability of the *FLH1*-transfected cells was less than that of the control cells. Two independent wound healing assays showed significant wound healing inhibition after 12-h incubation in the *FHL-1* transfected cells compared to the control cells (45.78±6.2 and 100±0, respectively; $p<0.009$) (Fig. 5B). Next, we evaluated the invasive capacity of the BC cell lines using an *in vitro* invasion assay since penetration of extracellular matrix and basement membrane by cancer cells is a key step in tumor invasion. As shown in Fig. 6A, there were fewer invading cells in the *FHL1*-transfected cells than in the control cells. The number of invading cells was significantly lower in the *FHL1*-transfected cells than in the control cells (18.5±2.3 and 95.2±2.4, respectively; $p=0.02$) (Fig. 6B).

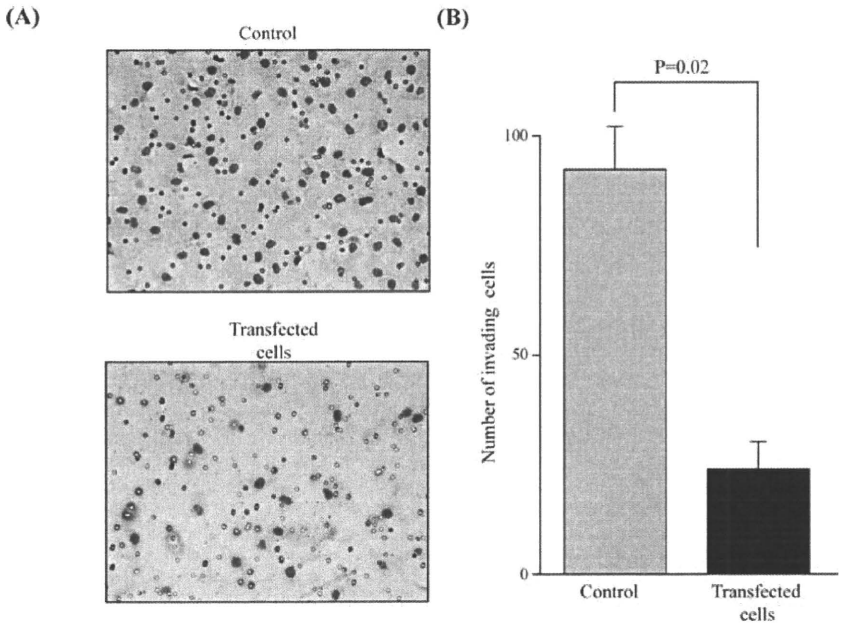

Figure 6. Effect of *FHL1* transfection on cell invasion. (A) Representative photographs of cell invasion activity from the Matrigel invasion assay. Number of invading cells was lower in *FHL1*-transfected cells than in control cells. (B) Number of invading cells counted in four random fields (mean ± SD). *FHL1*-transfected cells had significantly fewer invading cells.

Discussion

The four-and-a-half LIM (FHL) proteins are characterized by four complete LIM domains preceded by an N-terminal half LIM domain. LIM domains are cysteine-rich zinc finger motifs involved in a wide range of protein-protein interactions (17). Through interaction with cellular proteins, FHL proteins regulate cellular processes, including proliferation, differentiation, apoptosis, adhesion, migration, transcription, and signal transduction (18-22). Among these *FHL* family genes, we focused on *FHL1*, which was selected on the basis of two types of microarray analysis (3,4). Although the down-regulation of *FHL1* has been found in several types of cancer (9-13), the expression level and molecular function of *FHL1* in BC have not been clarified. Since many tumor suppressor genes silenced by DNA methylation have been identified in primary BC samples (14,15), we hypothesized that *FHL1* expression is down-regulated by promoter hypermethylation in BC cells and that *FHL1* functions as a tumor suppressor in BC cells.

In this study, we found that *FHL1* was significantly down-regulated at the mRNA level in the human BC tissue samples and that the methylation index was significantly higher in BC specimens than in NBE ones. Treatment with demethylation agent (5-aza-dC) restored *FHL1* mRNA expression in the BC cell lines. These results suggest that the down-regulation of *FHL1* expression in BC cell lines and human BC tissue correlates with CpG hypermethylation of the *FHL1* promoter. This is in accordance with our initial hypothesis that the *FHL1* promoter region is hypermethylated in BC. Since there was no apparent relationship between the clinicopathological parameters and the *FHL1* methylation index or mRNA expression, promoter methylation and down-regulation of *FHL1* might be involved in the initial stage of tumorigenesis (23).

We also hypothesized that *FHL1* functions as a tumor suppressor in BC. To examine the function of the *FHL1* gene, we established stable *FHL1*-transfected cells and compared their proliferation, migration, and invasion activities with those of the control BOY cell line, which was transfected with an empty vector. Cell proliferation assay revealed no difference in cell growth ability between the *FHL1*-transfected cells and the control cells. Shen *et al* demonstrated that *FHL1*-transfected cells have lower activity of non-anchored cell growth but not of anchored cell growth (9). Although the difference in the cell growth mechanism between anchored and non-anchored cells is unknown, our finding is similar to theirs. Although *FHL1* restoration resulted in no significant difference on anchored cell growth, we demonstrated that it significantly inhibited cell migration and invasion. These results strongly indicate that *FHL1* functions as a tumor suppressor in BC cells. Ding *et al* demonstrated that transfection of hepatocellular cancer cell line HepG2 with *FHL1* inhibited cell growth and decreased anchorage-independent colony formation whereas *FHL1* knockdown by siRNA increased cell growth and colony formation (17). They also found that FHL proteins ultimately increased the expression of growth inhibitor genes, such as the CDK inhibitor, *p21*, and that they decreased the expression of the growth-promoting gene, *c-myc* (17). In addition, *FHL1* interacts with estrogen receptors and inhibits breast cancer cell growth (24,25). Moreover, estrogen receptors are highly expressed in BC and contribute to BC cell proliferation (26,27). Thus, previous and current findings lead us to think that *FHL1* might have a tumor suppressive function through interaction with p21, c-myc, and estrogen receptors in BC. Further study is necessary to test this hypothesis.

In conclusion, we have shown that *FHL1* is frequently down-regulated in BC cell lines and clinical BC tissue. The mechanism of *FHL1* down-regulation in BC is through CpG hypermethylation of the promoter region. In addition, *FHL1* restoration causes suppression of BC cell migration and invasion. These results suggest that *FHL1* functions as a tumor suppressor gene in BC cells and that restoration of *FHL1* might offer a new therapeutic approach for the treatment of BC patients.

Acknowledgements

We thank Ms. M. Miyazaki for her excellent laboratory assistance.

References

1. Jemal A, Siegel R, Ward E, *et al*: Cancer statistics, 2008. CA Cancer J Clin 58: 71-96, 2008.
2. Mitra AP, Datar RH and Cote RJ: Molecular pathways in invasive bladder cancer: new insights into mechanisms, progression, and target identification. J Clin Oncol 24: 5552-5564, 2006.
3. Kawakami K, Enokida H, Tachiwada T, *et al*: Identification of differentially expressed genes in human bladder cancer through genome-wide gene expression profiling. Oncol Rep 16: 521-531, 2006.
4. Mori K, Enokida H, Kagara I, *et al*: CpG hypermethylation of collagen type I alpha 2 contributes to proliferation and migration activity of human bladder cancer. Int J Oncol 34: 1593-1602, 2009.
5. Johannessen M, Moller S, Hansen T, *et al*: The multifunctional roles of the four-and-a-half-LIM only protein FHL2. Cell Mol Life Sci 63: 268-284, 2006.
6. Morgan MJ, Madgwick AJ, Charleston B, *et al*: The developmental regulation of a novel muscle LIM-protein. Biochem Biophys Res Commun 212: 840-846, 1995.
7. Brown S, McGrath MJ, Ooms LM, *et al*: Characterization of two isoforms of the skeletal muscle LIM protein 1, SLIM1. J Biol Chem 274: 27083-27089, 1999.
8. Oku N, Sasabe E, Ueta E, *et al*: Tight junction protein claudin-1 enhances the invasive activity of oral squamous cell carcinoma cells by promoting cleavage of laminin-5 c2 chain via matrix metalloproteinase (MMP)-2 and membrane-type MMP-1. Cancer Res 66: 5251-5257, 2006.
9. Shen Y, Jia Z, Nagele RG, *et al*: Src uses Cas to suppress Fhl1 in order to promote nonanchored growth and migration of tumor cells. Cancer Res 66: 1543-1552, 2006.
10. Bhattacharjee A, Richards WG, Staunton J, *et al*: Classification of human lung carcinomas by mRNA expression profiling reveals distinct adenocarcinoma subclasses. Proc Natl Acad Sci USA 98: 13790-13795, 2001.
11. Fryknäs M, Wickenberg-Bolin U, Göransson H, *et al*: Molecular markers for discrimination of benign and malignant follicular thyroid tumors. Tumor Biol 27: 211-220, 2006.
12. Sakashita K, Mimori K, Tanaka F, *et al*: Clinical significance of loss of Fhl1 expression in human gastric cancer. Ann Surg Oncol 15: 2293-2300, 2008.
13. Li X, Jia Z, Shen Y, Ichikawa H, Jarvik J, Nagele RG and Goldberg GS: Coordinate suppression of Sdpr and Fhl1 expression in tumors of the breast, kidney, and prostate. Cancer Sci 99: 1326-1333, 2008.
14. Enokida H and Nakagawa M: Epigenetics in bladder cancer. Int J Clin Oncol 13: 298-307, 2008.